

Robust Bayesian Cluster Enumeration

Freywini K. Teklehaymanot, *Student Member, IEEE*, Michael Muma, *Member, IEEE*,
and Abdelhak M. Zoubir, *Fellow, IEEE*

Abstract—A major challenge in cluster analysis is that the number of data clusters is mostly unknown and it must be estimated prior to clustering the observed data. In real-world applications, the observed data is often subject to heavy tailed noise and outliers which obscure the true underlying structure of the data. Consequently, estimating the number of clusters becomes challenging. To this end, we derive a robust cluster enumeration criterion by formulating the problem of estimating the number of clusters as maximization of the posterior probability of multivariate t_ν candidate models. We utilize Bayes' theorem and asymptotic approximations to come up with a robust criterion that possesses a closed-form expression. Further, we refine the derivation and provide a robust cluster enumeration criterion for the finite sample regime. The robust criteria require an estimate of cluster parameters for each candidate model as an input. Hence, we propose a two-step cluster enumeration algorithm that uses the expectation maximization algorithm to partition the data and estimate cluster parameters prior to the calculation of one of the robust criteria. The performance of the proposed algorithm is tested and compared to existing cluster enumeration methods using numerical and real data experiments.

Index Terms—robust, outlier, cluster enumeration, Bayesian information criterion, cluster analysis, unsupervised learning, multivariate t_ν distribution.

I. INTRODUCTION

CLUSTER analysis is an unsupervised learning task that finds the intrinsic structure in a set of unlabeled data by grouping similar objects into clusters. Cluster analysis plays a crucial role in a wide variety of fields of study, such as social sciences, biology, medical sciences, statistics, machine learning, pattern recognition, and computer vision [1]–[4]. A major challenge in cluster analysis is that the number of clusters is usually unknown but it is required to cluster the data. The estimation of the number of clusters, also called cluster enumeration, has attracted the interest of researchers for decades and various methods have been proposed in the literature, see for example [5]–[21] and the reviews in [4], [22]–[25]. However, to this day, no single best cluster enumeration method exists.

In real-world applications, the observed data is often subject to heavy tailed noise and outliers [3], [26]–[30] which obscure the true underlying structure of the data. Consequently, cluster enumeration becomes even more challenging when either the data is contaminated by a fraction of outliers or there exist deviations from the distributional assumptions. To this end, many robust cluster enumeration methods have been proposed

in the literature, see [27], [31]–[45] and the references therein. A popular approach in robust cluster analysis is to use the Bayesian information criterion (BIC), as derived by Schwarz [46], to estimate the number of data clusters after either removing outliers from the data [31]–[34], modeling noise or outliers using an additional component in a mixture modeling framework [35], [36], or exploiting the idea that the presence of outliers causes the distribution of the data to be heavy tailed and, subsequently, modeling the data as a mixture of heavy tailed distributions [37], [38]. For example, modeling the data using a family of t_ν distributions [47]–[53] provides a principled way of dealing with outliers by giving them less weight in the objective function. The family of t_ν distributions is flexible as it contains the heavy tailed Cauchy for $\nu = 1$ and the Gaussian distribution for $\nu \rightarrow \infty$ as special cases. Consequently, we model the clusters using a family of multivariate t_ν distributions and derive robust cluster enumeration criteria that account for outliers given that the degree of freedom parameter ν is sufficiently small.

In statistical model selection, it is known that the original BIC [46], [54] penalizes two structurally different models the same way if they have the same number of unknown parameters [55], [56]. Hence, careful examination of the original BIC is a necessity prior to its application in specific model selection problems [55]. Following this line of argument, we have recently derived the BIC for cluster analysis by formulating cluster enumeration as maximization of the posterior probability of candidate models [20], [21]. In [20] we showed that the BIC derived specifically for cluster enumeration has a different penalty term compared to the original BIC. However, robustness was not considered in [20], where a family of multivariate Gaussian candidate models were used to derive the criterion, which we refer to as BIC_N .

To the best of our knowledge, this is the first attempt made to derive a robust cluster enumeration criterion by formulating the cluster enumeration problem as maximization of the posterior probability of multivariate t_ν candidate models. Under some mild assumptions, we derive a robust Bayesian cluster enumeration criterion, BIC_{t_ν} . We show that BIC_{t_ν} has a different penalty term compared to the original BIC (BIC_{ot_ν}) [46], [54], given that the candidate models in the original BIC are represented by a family of multivariate t_ν distributions. Interestingly, for BIC_{t_ν} both the data fidelity and the penalty terms depend on the assumed distribution for the data, while for the original BIC changes in the data distribution only affect the data fidelity term. Asymptotically, BIC_{t_ν} converges to BIC_{ot_ν} . As a result, our derivations also provide a justification for the use of the original BIC with multivariate t_ν candidate models from a cluster analysis perspective. Further, we refine the derivation of BIC_t by providing an exact expression for its

F. K. Teklehaymanot and A. M. Zoubir are with the Signal Processing Group and the Graduate School of Computational Engineering, Technische Universität Darmstadt, Darmstadt, Germany (e-mail: ftekle@spg.tu-darmstadt.de; zoubir@spg.tu-darmstadt.de).

M. Muma is with the Signal Processing Group, Technische Universität Darmstadt, Darmstadt, Germany (e-mail: muma@spg.tu-darmstadt.de).

penalty term. This results in a robust criterion, $\text{BIC}_{\text{ft}\nu}$, which behaves better than $\text{BIC}_{t\nu}$ in the finite sample regime and converges to $\text{BIC}_{t\nu}$ in the asymptotic regime.

In general, BIC based cluster enumeration methods require a clustering algorithm that partitions the data according to the number of clusters specified by each candidate model and provides an estimate of cluster parameters. Hence, we apply the expectation maximization (EM) algorithm to partition the data prior to the calculation of an enumeration criterion, resulting in a two-step approach. The proposed algorithm provides a unified framework for the robust estimation of the number of clusters and cluster memberships.

The paper is organized as follows. Section II formulates the cluster enumeration problem and Section III introduces the proposed robust cluster enumeration criterion. Section IV presents the two-step cluster enumeration algorithm. A comparison of different Bayesian cluster enumeration criteria is given in Section V. A performance evaluation and comparison to existing methods using numerical and real data experiments is provided in Section VI. Finally, Section VII contains concluding remarks and highlights future research directions. Notably, a detailed proof is provided in Appendix B.

Notation: Lower- and upper-case boldface letters represent column vectors and matrices, respectively; Calligraphic letters denote sets with the exception of \mathcal{L} which represents the likelihood function; \mathbb{R} , \mathbb{R}^+ , and \mathbb{Z}^+ denote the set of real numbers, the set of positive real numbers, and the set of positive integers, respectively; $p(\cdot)$ and $f(\cdot)$ denote probability mass function and probability density function (pdf), respectively; $\mathbf{x} \sim t_\nu(\boldsymbol{\mu}, \boldsymbol{\Psi})$ represents a multivariate t distributed random variable \mathbf{x} with location parameter $\boldsymbol{\mu}$, scatter matrix $\boldsymbol{\Psi}$, and degree of freedom ν ; $\hat{\boldsymbol{\theta}}$ denotes the estimator (or estimate) of the parameter $\boldsymbol{\theta}$; iid stands for independent and identically distributed; (A.) denotes an assumption; log stands for the natural logarithm; \mathbb{E} represents the expectation operator; \lim stands for the limit; $^\top$ represents vector or matrix transpose; $|\cdot|$ denotes the determinant when its argument is a matrix and an absolute value when its argument is scalar; \otimes represents the Kronecker product; $\text{vec}(\mathbf{Y})$ refers to the stacking of the columns of an arbitrary matrix \mathbf{Y} into a long column vector; $\mathcal{O}(1)$ denotes Landau's term which tends to a constant as the data size goes to infinity; \mathbf{I}_r stands for an $r \times r$ dimensional identity matrix; $\mathbf{0}_{r \times r}$ and $\mathbf{1}_{r \times r}$ represent an $r \times r$ dimensional all zero and all one matrix, respectively; $\#\mathcal{X}$ denotes the cardinality of the set \mathcal{X} ; \triangleq represents equality by definition; \equiv denotes mathematical equivalence.

II. PROBLEM FORMULATION

Let $\mathcal{X} \triangleq \{\mathbf{x}_1, \dots, \mathbf{x}_N\} \subset \mathbb{R}^{r \times N}$ denote the observed data set which can be partitioned into K independent, mutually exclusive, and non-empty clusters $\{\mathcal{X}_1, \dots, \mathcal{X}_K\}$. Each cluster \mathcal{X}_k , for $k \in \mathcal{K} \triangleq \{1, \dots, K\}$, contains N_k data vectors that are realizations of iid multivariate t_ν random variables $\mathbf{x}_k \sim t_{\nu_k}(\boldsymbol{\mu}_k, \boldsymbol{\Sigma}_k)$, where $\boldsymbol{\mu}_k \in \mathbb{R}^{r \times 1}$, $\boldsymbol{\Psi}_k \in \mathbb{R}^{r \times r}$, and $\nu_k \in \mathbb{R}^+$ represent the centroid, the scatter matrix, and the degree of freedom of the k th cluster, respectively. Let $\mathcal{M} \triangleq \{M_{L_{\min}}, \dots, M_{L_{\max}}\}$ be a family of multivariate t_ν

candidate models, where L_{\min} and L_{\max} represent the specified minimum and maximum number of clusters, respectively. Each candidate model $M_l \in \mathcal{M}$, for $l = L_{\min}, \dots, L_{\max}$ and $l \in \mathbb{Z}^+$, represents a partition of \mathcal{X} into l clusters with associated cluster parameter matrix $\boldsymbol{\Theta}_l = [\boldsymbol{\theta}_1, \dots, \boldsymbol{\theta}_l]$, which lies in a parameter space $\Omega_l \subset \mathbb{R}^{q \times l}$. Assuming that

(A.1) the degree of freedom parameter ν_m , for $m = 1, \dots, l$, is fixed at some prespecified value,

the parameters of interest reduce to $\boldsymbol{\theta}_m = [\boldsymbol{\mu}_m, \boldsymbol{\Psi}_m]^\top$. Our research goal is to estimate the number of clusters in \mathcal{X} given \mathcal{M} assuming that

(A.2) the constraint $L_{\min} \leq K \leq L_{\max}$ is satisfied.

Note that, given some mild assumptions are satisfied, we have recently derived a general Bayesian cluster enumeration criterion, which we refer to as BIC_G [20]. However, since we assume multivariate t_ν candidate models, some of the assumptions made in the derivation of BIC_G require mathematical justification. In the next section, we highlight the specific assumptions that require justification and, in an attempt to keep the article self contained, provide all necessary derivations.

III. ROBUST BAYESIAN CLUSTER ENUMERATION CRITERION

Our objective is to select a model $M_{\hat{K}}$ which is a posteriori most probable among the set of candidate models \mathcal{M} . Mathematically

$$M_{\hat{K}} = \arg \max_{\mathcal{M}} p(M_l | \mathcal{X}), \quad (1)$$

where $p(M_l | \mathcal{X})$ is the posterior probability of M_l given \mathcal{X} , which can be written as

$$p(M_l | \mathcal{X}) = \int_{\Omega_l} f(M_l, \boldsymbol{\Theta}_l | \mathcal{X}) d\boldsymbol{\Theta}_l, \quad (2)$$

where $f(M_l, \boldsymbol{\Theta}_l | \mathcal{X})$ denotes the joint posterior density of M_l and $\boldsymbol{\Theta}_l$ given \mathcal{X} . According to Bayes' theorem

$$f(M_l, \boldsymbol{\Theta}_l | \mathcal{X}) = \frac{p(M_l) f(\boldsymbol{\Theta}_l | M_l) \mathcal{L}(\boldsymbol{\Theta}_l | \mathcal{X})}{f(\mathcal{X})}, \quad (3)$$

where $p(M_l)$ denotes a discrete prior on $M_l \in \mathcal{M}$, $f(\boldsymbol{\Theta}_l | M_l)$ represents the prior on $\boldsymbol{\Theta}_l$ given M_l , $f(\mathcal{X})$ denotes the pdf of the data set \mathcal{X} , and $\mathcal{L}(\boldsymbol{\Theta}_l | \mathcal{X}) \triangleq f(\mathcal{X} | M_l, \boldsymbol{\Theta}_l)$ is the likelihood function. Substituting Eq. (3) into Eq. (2) results in

$$p(M_l | \mathcal{X}) = f(\mathcal{X})^{-1} p(M_l) \int_{\Omega_l} f(\boldsymbol{\Theta}_l | M_l) \mathcal{L}(\boldsymbol{\Theta}_l | \mathcal{X}) d\boldsymbol{\Theta}_l. \quad (4)$$

Since

$$\arg \max_{\mathcal{M}} p(M_l | \mathcal{X}) \equiv \arg \max_{\mathcal{M}} \log p(M_l | \mathcal{X}), \quad (5)$$

we maximize $\log p(M_l | \mathcal{X})$ over the family of candidate models \mathcal{M} for mathematical convenience. Hence, taking the natural logarithm of Eq. (4) results in

$$\log p(M_l | \mathcal{X}) = \log p(M_l) + \log \int_{\Omega_l} f(\boldsymbol{\Theta}_l | M_l) \mathcal{L}(\boldsymbol{\Theta}_l | \mathcal{X}) d\boldsymbol{\Theta}_l + \rho, \quad (6)$$

where $\rho = -\log f(\mathcal{X})$ is a constant that is independent of M_l and, consequently, has no effect on the maximization of

$\log p(M_l|\mathcal{X})$ over \mathcal{M} . As the partitions (clusters) $\mathcal{X}_m \subseteq \mathcal{X}$, for $m = 1, \dots, l$, are independent, mutually exclusive, and non-empty, the following holds:

$$f(\Theta_l|M_l) = \prod_{m=1}^l f(\theta_m|M_l) \quad (7)$$

$$\mathcal{L}(\Theta_l|\mathcal{X}) = \prod_{m=1}^l \mathcal{L}(\theta_m|\mathcal{X}_m) \quad (8)$$

Substituting Eqs. (7) and (8) into Eq. (6) results in

$$\log p(M_l|\mathcal{X}) = \log p(M_l) + \sum_{m=1}^l \log \int_{\mathbb{R}^q} f(\theta_m|M_l) \mathcal{L}(\theta_m|\mathcal{X}_m) d\theta_m + \rho. \quad (9)$$

Maximization of Eq. (9) over \mathcal{M} involves the maximization of the natural logarithm of a multidimensional integral. The multidimensional integral can be solved using either numerical integration or asymptotic approximations that result in a closed-form solution. Closed-form solutions are known to provide an insight into the model selection problem at hand [55]. Hence, we apply Laplace's method of integration [20], [55]–[57], which makes asymptotic approximations, to simplify the multidimensional integral in Eq. (9).

For ease of notation, Eq. (9) is written as

$$\log p(M_l|\mathcal{X}) = \log p(M_l) + \sum_{m=1}^l \log U + \rho, \quad (10)$$

where

$$U \triangleq \int_{\mathbb{R}^q} f(\theta_m|M_l) \exp(\log \mathcal{L}(\theta_m|\mathcal{X}_m)) d\theta_m. \quad (11)$$

Given that

(A.3) $\log \mathcal{L}(\theta_m|\mathcal{X}_m)$, for $m = 1, \dots, l$, has first- and second-order derivatives that are continuous over the parameter space Ω_l ,

(A.4) $\log \mathcal{L}(\theta_m|\mathcal{X}_m)$, for $m = 1, \dots, l$, has global maximum at $\hat{\theta}_m$, where $\hat{\theta}_m$ is an interior point of Ω_l , and

(A.5) the Hessian matrix of $-\frac{1}{N_m} \log \mathcal{L}(\theta_m|\mathcal{X}_m)$, which is given by

$$\hat{\mathbf{H}}_m \triangleq -\frac{1}{N_m} \frac{d^2 \log \mathcal{L}(\theta_m|\mathcal{X}_m)}{d\theta_m d\theta_m^\top} \Big|_{\theta_m=\hat{\theta}_m} \in \mathbb{R}^{q \times q},$$

where N_m is the cardinality of \mathcal{X}_m ($N_m = \#\mathcal{X}_m$), is positive definite for $m = 1, \dots, l$,

$\log \mathcal{L}(\theta_m|\mathcal{X}_m)$ can be approximated by its second-order Taylor series expansion around $\hat{\theta}_m$ as follows:

$$\begin{aligned} \log \mathcal{L}(\theta_m|\mathcal{X}_m) &\approx \log \mathcal{L}(\hat{\theta}_m|\mathcal{X}_m) + \tilde{\theta}_m^\top \frac{d \log \mathcal{L}(\theta_m|\mathcal{X}_m)}{d\theta_m} \Big|_{\theta_m=\hat{\theta}_m} \\ &\quad + \frac{1}{2} \tilde{\theta}_m^\top \left[\frac{d^2 \log \mathcal{L}(\theta_m|\mathcal{X}_m)}{d\theta_m d\theta_m^\top} \Big|_{\theta_m=\hat{\theta}_m} \right] \tilde{\theta}_m \\ &= \log \mathcal{L}(\hat{\theta}_m|\mathcal{X}_m) - \frac{N_m}{2} \tilde{\theta}_m^\top \hat{\mathbf{H}}_m \tilde{\theta}_m, \end{aligned} \quad (12)$$

where $\tilde{\theta}_m \triangleq \theta_m - \hat{\theta}_m$. The first derivative of $\log \mathcal{L}(\theta_m|\mathcal{X}_m)$ evaluated at $\hat{\theta}_m$ vanishes because of assumption **(A.4)**.

Note that $\log \mathcal{L}(\theta_m|\mathcal{X}_m)$, for $m = 1, \dots, l$, is known to have multiple local maxima [51], [53]. For assumption **(A.4)** to hold, we have to show that $\hat{\theta}_m$ is the global maximum of $\log \mathcal{L}(\theta_m|\mathcal{X}_m)$, for $m = 1, \dots, l$. We know that the global maximizer of $\log \mathcal{L}(\theta_m|\mathcal{X}_m)$, is θ_m^0 , where θ_m^0 is the true parameter vector. $\hat{\theta}_m$ is the maximum likelihood estimator and its derivation and the final expressions are given in Appendix A. In [58], it was proven that

$$\lim_{N_m \rightarrow \infty} \hat{\theta}_m = \theta_m^0$$

with probability one. As a result, asymptotically, assumption **(A.4)** holds. Assumption **(A.5)** follows because $\hat{\theta}_m$ is a maximizer of $\log \mathcal{L}(\theta_m|\mathcal{X}_m)$.

Assume that

(A.6) $f(\theta_m|M_l)$, for $m = 1, \dots, l$, is continuously differentiable and its first-order derivatives are bounded on Ω_l with $f(\hat{\theta}_m|M_l) \neq 0$.

Then, substituting Eq. (12) into Eq. (11) and approximating $f(\theta_m|M_l)$ by its Taylor series expansion yields

$$\begin{aligned} U &\approx \int_{\mathbb{R}^q} \left(\left[f(\hat{\theta}_m|M_l) + \tilde{\theta}_m^\top \frac{df(\theta_m|M_l)}{d\theta_m} \Big|_{\theta_m=\hat{\theta}_m} + \text{HOT} \right] \right. \\ &\quad \left. \times \mathcal{L}(\hat{\theta}_m|\mathcal{X}_m) \exp\left(-\frac{N_m}{2} \tilde{\theta}_m^\top \hat{\mathbf{H}}_m \tilde{\theta}_m\right) d\theta_m \right), \end{aligned} \quad (13)$$

where HOT denotes higher order terms and $\exp\left(-\frac{N_m}{2} \tilde{\theta}_m^\top \hat{\mathbf{H}}_m \tilde{\theta}_m\right)$ is a Gaussian kernel with mean $\hat{\theta}_m$ and covariance matrix $(N_m \hat{\mathbf{H}}_m)^{-1}$. Ignoring the higher order terms, Eq. (13) reduces to

$$\begin{aligned} U &\approx f(\hat{\theta}_m|M_l) \mathcal{L}(\hat{\theta}_m|\mathcal{X}_m) \int_{\mathbb{R}^q} \exp\left(-\frac{N_m}{2} \tilde{\theta}_m^\top \hat{\mathbf{H}}_m \tilde{\theta}_m\right) d\theta_m \\ &\quad + \int_{\mathbb{R}^q} \tilde{\theta}_m^\top \frac{df(\theta_m|M_l)}{d\theta_m} \Big|_{\theta_m=\hat{\theta}_m} \mathcal{L}(\hat{\theta}_m|\mathcal{X}_m) \\ &\quad \times \exp\left(-\frac{N_m}{2} \tilde{\theta}_m^\top \hat{\mathbf{H}}_m \tilde{\theta}_m\right) d\theta_m. \end{aligned} \quad (14)$$

The second term in Eq. (14) is equivalent to $\kappa \mathbb{E}[\theta_m - \hat{\theta}_m] = 0$, where $\kappa < \infty$ is a constant. Consequently, Eq. (14) reduces to

$$\begin{aligned} U &\approx f(\hat{\theta}_m|M_l) \mathcal{L}(\hat{\theta}_m|\mathcal{X}_m) \int_{\mathbb{R}^q} \exp\left(-\frac{N_m}{2} \tilde{\theta}_m^\top \hat{\mathbf{H}}_m \tilde{\theta}_m\right) d\theta_m \\ &= f(\hat{\theta}_m|M_l) \mathcal{L}(\hat{\theta}_m|\mathcal{X}_m) \int_{\mathbb{R}^q} \left((2\pi)^{q/2} |N_m^{-1} \hat{\mathbf{H}}_m^{-1}|^{1/2} \right. \\ &\quad \left. \frac{1}{(2\pi)^{q/2} |N_m^{-1} \hat{\mathbf{H}}_m^{-1}|^{1/2}} \exp\left(-\frac{N_m}{2} \tilde{\theta}_m^\top \hat{\mathbf{H}}_m \tilde{\theta}_m\right) d\theta_m \right) \\ &= f(\hat{\theta}_m|M_l) \mathcal{L}(\hat{\theta}_m|\mathcal{X}_m) (2\pi)^{q/2} |N_m^{-1} \hat{\mathbf{H}}_m^{-1}|^{1/2} \end{aligned} \quad (15)$$

given that $N_m \rightarrow \infty$. Substituting Eq. (15) into Eq. (10) results in

$$\begin{aligned} \log p(M_l|\mathcal{X}) &\approx \log p(M_l) + \sum_{m=1}^l \log \left(f(\hat{\theta}_m|M_l) \mathcal{L}(\hat{\theta}_m|\mathcal{X}_m) \right) \\ &\quad + \frac{lq}{2} \log 2\pi - \frac{1}{2} \sum_{m=1}^l \log |\hat{\mathbf{J}}_m| + \rho, \end{aligned} \quad (16)$$

where

$$\hat{\mathbf{J}}_m \triangleq N_m \hat{\mathbf{H}}_m = - \left. \frac{d^2 \log \mathcal{L}(\boldsymbol{\theta}_m | \mathcal{X}_m)}{d\boldsymbol{\theta}_m d\boldsymbol{\theta}_m^\top} \right|_{\boldsymbol{\theta}_m = \hat{\boldsymbol{\theta}}_m} \quad (17)$$

is the Fisher information matrix (FIM) of the data vectors that belong to the m th partition.

IV. PROPOSED ROBUST BAYESIAN CLUSTER ENUMERATION ALGORITHM

We propose a robust cluster enumeration algorithm to estimate the number of clusters in the data set \mathcal{X} . The presented two-step approach utilizes an unsupervised learning algorithm to partition \mathcal{X} into the number of clusters specified by each candidate model $M_l \in \mathcal{M}$ prior to the computation of one of the proposed robust cluster enumeration criteria for that particular model.

A. Proposed Robust Bayesian Cluster Enumeration Criteria

For each candidate model $M_l \in \mathcal{M}$, let there be a clustering algorithm that partitions \mathcal{X} into l clusters and provides parameter estimates $\hat{\boldsymbol{\theta}}_m = [\hat{\boldsymbol{\mu}}_m, \hat{\boldsymbol{\Psi}}_m]^\top$, for $m = 1, \dots, l$. Assume that (A.1)-(A.7) are fulfilled.

Theorem 1. *The posterior probability of M_l given \mathcal{X} can be asymptotically approximated by*

$$\begin{aligned} \text{BIC}_{t_\nu}(M_l) &\triangleq \log p(M_l | \mathcal{X}) \\ &\approx \log \mathcal{L}(\hat{\boldsymbol{\Theta}}_l | \mathcal{X}) - \frac{q}{2} \sum_{m=1}^l \log \epsilon, \end{aligned} \quad (18)$$

where $q = \frac{1}{2}r(r+3)$ represents the number of estimated parameters per cluster and

$$\epsilon = \max \left(\sum_{\mathbf{x}_n \in \mathcal{X}_m} w_n^2, N_m \right). \quad (19)$$

The likelihood function, also called the data fidelity term, is given by

$$\begin{aligned} \log \mathcal{L}(\hat{\boldsymbol{\Theta}}_l | \mathcal{X}) &\approx \sum_{m=1}^l N_m \log N_m - \sum_{m=1}^l \frac{N_m}{2} \log |\hat{\boldsymbol{\Psi}}_m| \\ &+ \sum_{m=1}^l N_m \log \frac{\Gamma((\nu_m + r)/2)}{\Gamma(\nu_m/2) (\pi \nu_m)^{r/2}} \\ &- \frac{1}{2} \sum_{m=1}^l \sum_{\mathbf{x}_n \in \mathcal{X}_m} (\nu_m + r) \log \left(1 + \frac{\delta_n}{\nu_m} \right), \end{aligned} \quad (20)$$

where $N_m = \#\mathcal{X}_m$, $\Gamma(\cdot)$ denotes the gamma function, and $\delta_n = (\mathbf{x}_n - \hat{\boldsymbol{\mu}}_m)^\top \hat{\boldsymbol{\Psi}}_m^{-1} (\mathbf{x}_n - \hat{\boldsymbol{\mu}}_m)$ is the squared Mahalanobis distance. The second term in the second line of Eq. (18) is referred to as the penalty term.

Proof. Proving that Eq. (16) reduces to Eq. (18) requires approximating $|\hat{\mathbf{J}}_m|$ and, consequently, writing a closed-form expression for $\text{BIC}_{t_\nu}(M_l)$. A detailed proof is given in Appendix B. \blacksquare

Once $\text{BIC}_{t_\nu}(M_l)$ is computed for each candidate model $M_l \in \mathcal{M}$, the number of clusters in \mathcal{X} is estimated as

$$\hat{K}_{\text{BIC}_{t_\nu}} = \arg \max_{l=L_{\min}, \dots, L_{\max}} \text{BIC}_{t_\nu}(M_l). \quad (21)$$

Corollary 1. *When the data size is finite, one can opt to compute $\log |\hat{\mathbf{J}}_m|$, without asymptotic approximations to obtain a more accurate penalty term. In such cases, the posterior probability of M_l given \mathcal{X} becomes*

$$\text{BIC}_{\text{Ft}_\nu}(M_l) \approx \log \mathcal{L}(\hat{\boldsymbol{\Theta}}_l | \mathcal{X}) - \frac{1}{2} \sum_{m=1}^l \log |\hat{\mathbf{J}}_m|, \quad (22)$$

where the expression for $|\hat{\mathbf{J}}_m|$ is given in Appendix C.

B. The Expectation Maximization (EM) Algorithm for t_ν Mixture Models

We consider maximum likelihood estimation of the parameters of the l -component mixture of t_ν distributions

$$f(\mathbf{x}_n | M_l, \boldsymbol{\Phi}_l) = \sum_{m=1}^l \tau_m g(\mathbf{x}_n; \boldsymbol{\mu}_m, \boldsymbol{\Psi}_m, \nu_m), \quad (23)$$

where $g(\mathbf{x}_n; \boldsymbol{\mu}_m, \boldsymbol{\Psi}_m, \nu_m)$ denotes the r -variate t_ν pdf and $\boldsymbol{\Phi}_l = [\boldsymbol{\tau}_l, \boldsymbol{\Theta}_l^\top, \boldsymbol{\nu}_l]$. $\boldsymbol{\tau}_l = [\tau_1, \dots, \tau_l]^\top$ are the mixing coefficients and $\boldsymbol{\nu}_l = [\nu_1, \dots, \nu_l]^\top$ are assumed to be known or estimated, e.g. using [48]. The mixing coefficients satisfy the constraints $0 < \tau_m < 1$ for $m = 1, \dots, l$, and $\sum_{m=1}^l \tau_m = 1$.

The EM algorithm is widely used to estimate the parameters of the l -component mixture of t_ν distributions [47]–[49], [59]. The EM algorithm contains two basic steps, namely the E step and the M step, which are performed iteratively until a convergence condition is satisfied. The E step computes

$$\hat{v}_{nm}^{(i)} = \frac{\hat{\tau}_m^{(i-1)} g(\mathbf{x}_n; \boldsymbol{\mu}_m^{(i-1)}, \boldsymbol{\Psi}_m^{(i-1)}, \nu_m)}{\sum_{j=1}^l \hat{\tau}_j^{(i-1)} g(\mathbf{x}_n; \boldsymbol{\mu}_j^{(i-1)}, \boldsymbol{\Psi}_j^{(i-1)}, \nu_j)} \quad (24)$$

$$\hat{w}_{nm}^{(i)} = \frac{\nu_m + r}{\nu_m + \delta_n^{(i-1)}}, \quad (25)$$

where $\hat{v}_{nm}^{(i)}$ is the posterior probability that \mathbf{x}_n belongs to the m th cluster at the i th iteration and $\hat{w}_{nm}^{(i)}$ is the weight given to \mathbf{x}_n by the m th cluster at the i th iteration. Once $\hat{v}_{nm}^{(i)}$ and $\hat{w}_{nm}^{(i)}$ are calculated, the M step updates cluster parameters as follows:

$$\hat{\tau}_m^{(i)} = \frac{\sum_{n=1}^N \hat{v}_{nm}^{(i)}}{N} \quad (26)$$

$$\hat{\boldsymbol{\mu}}_m^{(i)} = \frac{\sum_{n=1}^N \hat{v}_{nm}^{(i)} w_{nm}^{(i)} \mathbf{x}_n}{\sum_{n=1}^N \hat{v}_{nm}^{(i)} w_{nm}^{(i)}} \quad (27)$$

$$\hat{\boldsymbol{\Psi}}_m^{(i)} = \frac{\sum_{n=1}^N \hat{v}_{nm}^{(i)} w_{nm}^{(i)} (\mathbf{x}_n - \hat{\boldsymbol{\mu}}_m^{(i)}) (\mathbf{x}_n - \hat{\boldsymbol{\mu}}_m^{(i)})^\top}{\sum_{n=1}^N \hat{v}_{nm}^{(i)}} \quad (28)$$

Algorithm 1 summarizes the working principle of the proposed robust two-step cluster enumeration approach. Given that the degree of freedom parameter ν is fixed at some finite value, the computational complexity of Algorithm 1 is the sum of the run times of the two steps. Since the initialization, i.e., the K-medians algorithm is performed only for a few iterations,

the computational complexity of the first step is dominated by the EM algorithm and it is given by $\mathcal{O}(Nr^2li_{\max})$ for a single candidate model M_l , where i_{\max} is a fixed stopping threshold of the EM algorithm. The computational complexity of $\text{BIC}_{t_\nu}(M_l)$ is $\mathcal{O}(Nr^2)$, which is much smaller than the run-time of the EM algorithm and, as a result, it can easily be ignored in the run-time analysis of the proposed algorithm. Hence, the total computational complexity of Algorithm 1 is $\mathcal{O}(Nr^2(L_{\min} + \dots + L_{\max})i_{\max})$.

Note that if $\text{BIC}_{\text{ft}_\nu}(M_l)$ is used in Algorithm 1 instead of $\text{BIC}_{t_\nu}(M_l)$, the computational complexity of the algorithm increases significantly with the increase in the number of features (r) due to the calculation of Eq. (69).

Algorithm 1 Robust two-step cluster enumeration approach

Inputs: \mathcal{X} , L_{\min} , L_{\max} , and ν
for $l = L_{\min}, \dots, L_{\max}$ **do**
 Step 1: model-based clustering
 Step 1.1: the EM algorithm
 for $m = 1, \dots, l$ **do**
 Initialize $\hat{\mu}_m^0$ using the K-medians algorithm
 Initialize $\hat{\Psi}_m^0$ using the sample covariance estimator
 $\hat{\tau}_m^0 = \frac{N_m}{N}$
 end for
 for $i = 1, 2, \dots, i_{\max}$ **do**
 E step:
 for $n = 1, \dots, N$ **do**
 for $m = 1, \dots, l$ **do**
 Calculate $\hat{v}_{nm}^{(i)}$ using Eq. (24)
 Calculate $\hat{w}_{nm}^{(i)}$ using Eq. (25)
 end for
 end for
 M step:
 for $m = 1, \dots, l$ **do**
 Determine $\hat{\tau}_m^{(i)}$, $\hat{\mu}_m^{(i)}$, and $\hat{\Psi}_m^{(i)}$ via Eqs. (26)-(28)
 end for
 Check for the convergence of either $\hat{\Phi}_l^{(i)}$ or $\log \mathcal{L}(\hat{\Phi}_l^{(i)}|\mathcal{X})$
 if convergence condition is satisfied **then**
 Exit for loop
 end if
 end for
 Step 1.2: hard clustering
 for $n = 1, \dots, N$ **do**
 for $m = 1, \dots, l$ **do**

$$l_{nm} = \begin{cases} 1, & m = \arg \max_{j=1, \dots, l} \hat{v}_{nj}^{(i)} \\ 0, & \text{otherwise} \end{cases}$$

 end for
 end for
 for $m = 1, \dots, l$ **do**
 $N_m = \sum_{n=1}^N l_{nm}$
 end for
 Step 2: calculate $\text{BIC}_{t_\nu}(M_l)$ using Eq. (18)
end for
Estimate the number of clusters, $\hat{K}_{\text{BIC}_{t_\nu}}$, in \mathcal{X} via Eq. (21)

V. COMPARISON OF DIFFERENT BAYESIAN CLUSTER ENUMERATION CRITERIA

Model selection criteria that are derived by maximizing the posterior probability of candidate models given data are known to have a common form [20], [56], [60] that is consistent with

$$\log \mathcal{L}(\hat{\Theta}_l|\mathcal{X}) - \eta, \quad (29)$$

where $\log \mathcal{L}(\hat{\Theta}_l|\mathcal{X})$ is the data fidelity term and η is the penalty term. The proposed robust cluster enumeration criteria, BIC_{t_ν} and $\text{BIC}_{\text{ft}_\nu}$, and the original BIC with multivariate t_ν candidate models, $\text{BIC}_{\text{ot}_\nu}$, [37], [38], [48] have an identical data fidelity term. The difference in these criteria lies in their penalty terms, which are given by

$$\text{BIC}_{t_\nu} : \quad \eta = \frac{q}{2} \sum_{m=1}^l \log \epsilon \quad (30)$$

$$\text{BIC}_{\text{ft}_\nu} : \quad \eta = \frac{q}{2} \sum_{m=1}^l \log |\hat{J}_m| \quad (31)$$

$$\text{BIC}_{\text{ot}_\nu} : \quad \eta = \frac{ql}{2} \log N, \quad (32)$$

where ϵ and $|\hat{J}_m|$ are given by Eq. (19) and Eq. (69), respectively. Note that $\text{BIC}_{\text{ft}_\nu}$ calculates an exact value of the penalty term, while BIC_{t_ν} and $\text{BIC}_{\text{ot}_\nu}$ compute its asymptotic approximation. In the finite sample regime the penalty term of $\text{BIC}_{\text{ft}_\nu}$ is stronger than the penalty term of BIC_{t_ν} , while asymptotically all three criteria have an identical penalty term.

Remark. When the degree of freedom parameter $\nu \rightarrow \infty$ BIC_{t_ν} converges to

$$\begin{aligned} \text{BIC}_N(M_l) &\approx \sum_{m=1}^l N_m \log N_m - \sum_{m=1}^l \frac{N_m}{2} \log |\hat{\Sigma}_m| \\ &\quad - \frac{q}{2} \sum_{m=1}^l \log N_m, \end{aligned} \quad (33)$$

where BIC_N is the asymptotic criterion derived in [20] assuming a family of Gaussian candidate models.

Remark. A modification of the data distribution of the candidate models only affects the data fidelity term of the original BIC [46], [54]. However, given that the BIC is specifically derived for cluster analysis, we showed that both the data fidelity and penalty terms change as the data distribution of the candidate models changes, see Eq. (18) and the expression for BIC_N in [20].

A related robust cluster enumeration method that uses the original BIC to estimate the number of clusters is the trimmed BIC (TBIC) [32]. The TBIC estimates the number of clusters using Gaussian candidate models after trimming some percentage of the data. In TBIC, the fast trimmed likelihood estimator (FAST-TLE) is used to obtain maximum likelihood estimates of cluster parameters. The FAST-TLE is computationally expensive since it carries out a trial and a refinement step multiple times, see [32] for details.

VI. EXPERIMENTAL RESULTS

In this section, we compare the performance of the proposed robust two-step algorithm with state-of-the-art cluster enumeration methods using numerical and real data experiments. In addition to the methods discussed in Section V, we compare our cluster enumeration algorithm with the gravitational clustering (GC) [41] and the X-means [10] algorithms. All experimental results are an average of 300 Monte Carlo runs. The degree of freedom parameter is set to $\nu = 3$ for all methods that have multivariate t_ν candidate models. We use the author's implementation of the gravitational clustering algorithm [41]. For the TBIC, we trim 10% of the data and perform 10 iterations of the trial and refinement steps. For the model selection based methods, the minimum and maximum number of clusters is set to $L_{\min} = 1$ and $L_{\max} = 2K$, where K denotes the true number of clusters in the data under consideration.

A. Performance Measures

Performance is assessed in terms of the empirical probability of detection (p_{det}) and the mean absolute error (MAE), which are defined as

$$p_{\text{det}} = \frac{1}{I} \sum_{i=1}^I \mathbb{1}_{\{\hat{K}_i=K\}} \quad (34)$$

$$\text{MAE} = \frac{1}{I} \sum_{i=1}^I |K - \hat{K}_i|, \quad (35)$$

where I is the total number of Monte Carlo experiments, \hat{K}_i is the estimated number of clusters in the i th Monte Carlo experiment, and $\mathbb{1}_{\{\hat{K}_i=K\}}$ is the indicator function defined as

$$\mathbb{1}_{\{\hat{K}_i=K\}} \triangleq \begin{cases} 1, & \text{if } \hat{K}_i = K \\ 0, & \text{otherwise} \end{cases}. \quad (36)$$

In addition to these two performance measures, we also report the empirical probability of underestimation and overestimation, which are defined as

$$p_{\text{under}} = \frac{1}{I} \sum_{i=1}^I \mathbb{1}_{\{\hat{K}_i < K\}} \quad (37)$$

$$p_{\text{over}} = 1 - p_{\text{det}} - p_{\text{under}}, \quad (38)$$

respectively.

B. Numerical Experiments

1) *Analysis of the sensitivity of different cluster enumeration methods to outliers:* we generate two data sets which contain realizations of 2-dimensional random variables $\mathbf{x}_k \sim \mathcal{N}(\boldsymbol{\mu}_k, \boldsymbol{\Sigma}_k)$, where $k = 1, 2, 3$, with cluster centroids $\boldsymbol{\mu}_1 = [0, 5]^\top$, $\boldsymbol{\mu}_2 = [5, 0]^\top$, $\boldsymbol{\mu}_3 = [-5, 0]^\top$, and covariance matrices

$$\boldsymbol{\Sigma}_1 = \begin{bmatrix} 2 & 0.5 \\ 0.5 & 0.5 \end{bmatrix}, \boldsymbol{\Sigma}_2 = \begin{bmatrix} 1 & 0 \\ 0 & 0.1 \end{bmatrix}, \boldsymbol{\Sigma}_3 = \begin{bmatrix} 2 & -0.5 \\ -0.5 & 0.5 \end{bmatrix}.$$

The first data set (Data-1), as depicted in Fig. 1a, replaces a randomly selected data point with an outlier that is generated from a uniform distribution over the range $[-20, 20]$ on each

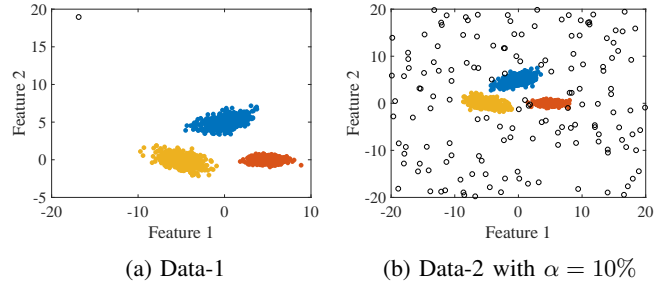


Fig. 1: Data-1 and Data-2 with $\alpha = 10\%$, where filled circles represent clean data and an open circle denotes an outlier.

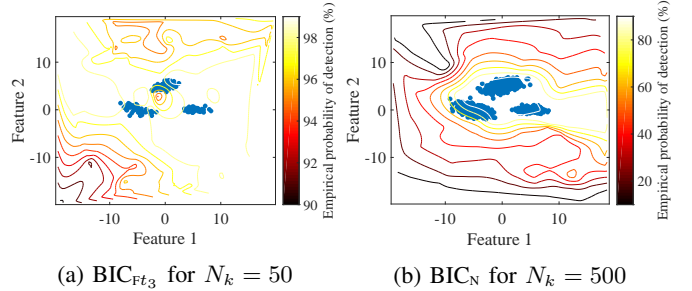


Fig. 2: Sensitivity curves of BIC_{Ft_3} and BIC_N at different values of N_k . The sensitivity curve demonstrates the sensitivity of a method to the presence of an outlier relative to its position.

variate at each iteration. The sensitivity of different cluster enumeration methods to a single replacement outlier over 100 iterations as a function of the number of data vectors per cluster (N_k) is displayed in Table I. From the compared methods, our robust criterion BIC_{Ft_3} has the best performance in terms of both p_{det} and MAE. Except for BIC_{Ft_3} and the TBIC, the performance of all methods deteriorates when N_k , for $k = 1, 2, 3$, is small and, notably, BIC_{t_3} performs poorly. This behavior is attributed to the fact that BIC_{t_3} is an asymptotic criterion and in the small sample regime its penalty term becomes weak which results in an increase in the empirical probability of overestimation. BIC_N and X-means are very sensitive to the presence of a single outlier because they model individual clusters as multivariate Gaussian. X-means performs even worse than BIC_N since it uses the K-means algorithm to cluster the data, which is ineffective in handling elliptical clusters. An illustrative example of the sensitivity of BIC_{Ft_3} and BIC_N to the presence of an outlier is displayed in Fig. 2. Despite the difference in N_k , when the outlier is either in one of the clusters or very close to one of the clusters, both BIC_{Ft_3} and BIC_N are able to estimate the correct number of clusters reasonably well. The difference between these two methods arises when the outlier is far away from the bulk of data. While BIC_{Ft_3} is still able to estimate the correct number of clusters, BIC_N starts to overestimate the number of clusters.

The second data set (Data-2), shown in Fig. 1b, contains $N_k = 500$ data points in each cluster k and replaces a certain percentage of the data set with outliers that are generated from a uniform distribution over the range $[-20, 20]$ on each variate.

TABLE I: The sensitivity of different cluster enumeration methods to the presence of a single replacement outlier as a function of the number of data points per cluster.

N_k		50	100	250	500
BIC_{t_3}	p_{det}	43.20	92.18	99.77	100
	MAE	1.28	0.11	0.002	0
BIC_{Ft_3}	p_{det}	96.89	100	100	100
	MAE	0.03	0	0	0
BIC_{Ot_3}	p_{det}	88.13	99.5	99.98	100
	MAE	0.18	0.005	0.0002	0
TBIC [32]	p_{det}	98.75	99.26	98.92	98.8
	MAE	0.013	0.008	0.01	0.01
GC [41]	p_{det}	73.07	94.85	99.80	100
	MAE	0.29	0.05	0.002	0
BIC_N [20]	p_{det}	10.92	15.60	33.82	42.20
	MAE	1.25	1.13	0.99	0.83
X-means [10]	p_{det}	1.24	1.17	1.38	0.17
	MAE	2.69	2.67	2.33	2.13

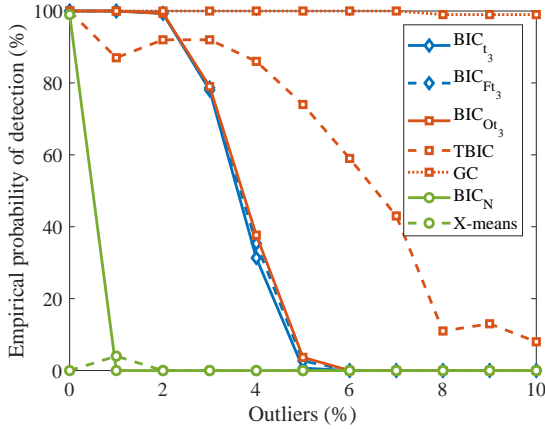


Fig. 3: The empirical probability of detection in % for Data-2 as a function of the percentage of outliers.

Data-2 is generated in a way that no outlier lies inside one of the data clusters. In this manner, we make sure that outliers are points that do not belong to the bulk of data. Fig. 3 shows the empirical probability of detection as a function of the percentage of outliers (α). GC is able to correctly estimate the number of clusters for $\alpha > 3\%$. The proposed robust criteria, BIC_{t_3} and BIC_{Ft_3} , and the original BIC, BIC_{Ot_3} , behave similarly and are able to estimate the correct number of clusters when $\alpha \leq 3\%$. The behavior of these methods is rather intuitive because as the amount of outliers increases, then the methods try to explain the outliers by opening a new cluster. A similar trend is observed for the TBIC even though its curve decays slowly. BIC_N is able to estimate the correct number of clusters 99% of the time when there are no outliers in the data set. However, even 1% of outliers is enough to drive BIC_N into overestimating the number of clusters.

2) *Impact of the increase in the number of features on the performance of cluster enumeration methods:* we generate realizations of the random variables $\mathbf{x}_k \sim t_3(\boldsymbol{\mu}_k, \boldsymbol{\Psi}_k)$, for $k = 1, 2$, whose cluster centroids and scatter matrices are given

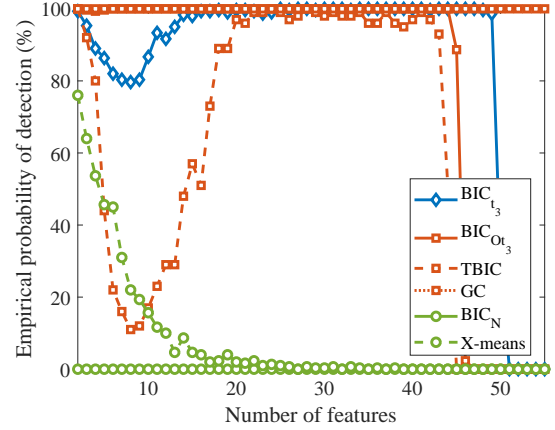


Fig. 4: The empirical probability of detection in % for Data-3 as a function of the number of features.

by

$$\boldsymbol{\mu}_k = c\mathbf{1}_{r \times 1}$$

$$\boldsymbol{\Psi}_k = \mathbf{I}_r,$$

with $c \in \{0, 15\}$, $\mathbf{1}_{r \times 1}$ denoting an r dimensional all one column vector, and \mathbf{I}_r representing an $r \times r$ dimensional identity matrix. For this data set, referred to as Data-3, the number of features r is varied in the range $r = 2, 3, \dots, 55$ and the number of data points per cluster is set to $N_k = 500$. Because $\nu = 3$, Data-3 contains realizations of heavy tailed distributions and, as a result, the clusters contain outliers. The empirical probability of detection as a function of the number of features is displayed in Fig. 4. The performance of GC appears to be invariant to the increase in the number of features, while the remaining methods are affected. But, compared to the other cluster enumeration methods, GC is computationally very expensive. BIC_{Ot_3} outperforms BIC_{t_3} and the TBIC when the number of features is low, while the proposed criterion BIC_{t_3} outperforms both methods in high dimensions. BIC_{Ft_3} is not computed for this data set because it is computationally expensive and it is not beneficial given the large number of samples.

3) *Analysis of the sensitivity of different cluster enumeration methods to cluster overlap:* here, we use Data-2 with 1% outliers and vary the distance between the second and the third centroid such that the percentage of overlap between the two clusters takes on a value from the set $\{0, 5, 10, 25, 50, 75, 100\}$. The empirical probability of detection as a function of the amount of overlap is depicted in Fig. 5. The best performance is achieved by BIC_{t_3} and BIC_{Ot_3} and, remarkably, both cluster enumeration criteria are able to correctly estimate the number of clusters even when there exists 75% overlap between the two clusters. As expected, when the amount of overlap is 100%, most methods underestimate the number of clusters to two. While it may appear that the enumeration performance of BIC_N increases for increasing amounts of overlap, in fact BIC_N groups the two overlapping clusters into one and attempts to explain the outliers by opening a new cluster. A similar trend is observed

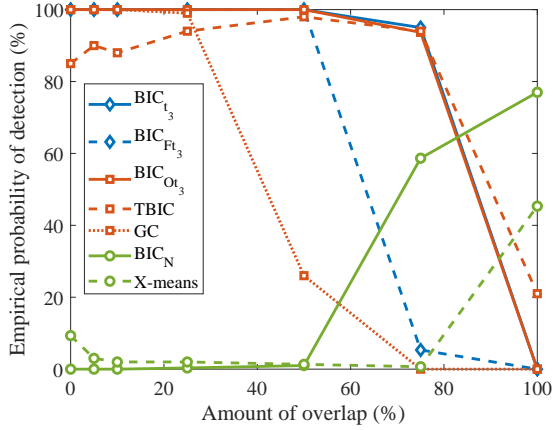


Fig. 5: Impact of cluster overlap on the performance of different cluster enumeration methods.

for X-means. GC is inferior to the other robust methods, and experiences an increase in the empirical probability of underestimation.

4) *Analysis of the sensitivity of cluster enumeration methods to cluster heterogeneity*: we generate realizations of 2-dimensional random variables $\mathbf{x}_k \sim t_3(\boldsymbol{\mu}_k, \boldsymbol{\Psi}_k)$, where the cluster centroids $\boldsymbol{\mu}_k$ are selected at random from a uniform distribution in the range $[-200, 200]$ in each variate and the scatter matrices are set to $\boldsymbol{\Psi}_k = \mathbf{I}_r$ for $k = 1, \dots, 5$. The data set is generated in a way that there is no overlap between the clusters. The number of data points in the first four clusters is set to $N_k = 500$, while N_5 is allowed to take on values from the set $\{500, 375, 250, 125, 50, 25, 5\}$. This data set (Data-4) contains multiple outliers since each cluster contains realizations of heavy tailed t distributed random variables. The empirical probability of detection as a function of the number of data points in the fifth cluster is shown in Fig. 6. The proposed cluster enumeration methods, BIC_{t_3} and BIC_{Ft_3} , are able to estimate the correct number of clusters with a high accuracy even when the fifth cluster contains only 1% of the data available in the other clusters. A similar performance is observed for BIC_{Ot_3} . TBIC and GC are slightly inferior in performance to the other robust cluster enumeration methods. When the number of data points in the fifth cluster increases, all robust methods perform well in estimating the number of clusters. Interestingly, X-means outperforms BIC_N since the considered clusters are all spherical. BIC_N overestimates the number of clusters and possesses the largest MAE.

C. Real Data Results

1) *Old Faithful geyser data set*: Old Faithful is a geyser located in Yellowstone National Park in Wyoming, United States. This data set, depicted in Fig. 7a, was used in the literature for density estimation [61], time series analysis [62], and cluster analysis [63], [64]. The performance of different cluster enumeration methods on the clean and contaminated versions of the Old Faithful data set is reported in Table II. The contaminated version, shown in Fig. 7b, is generated by replacing a randomly selected data point with an outlier at

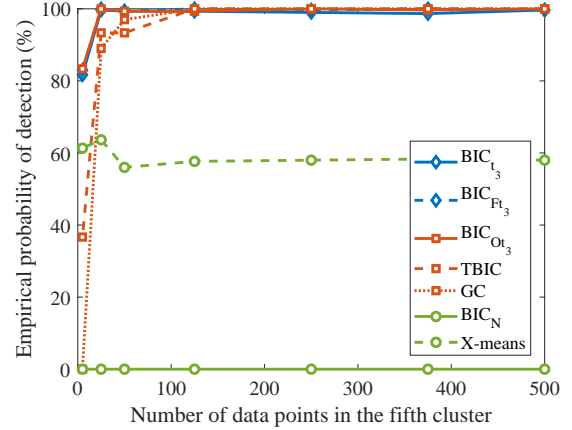


Fig. 6: Impact of cluster heterogeneity on the performance of different cluster enumeration methods.

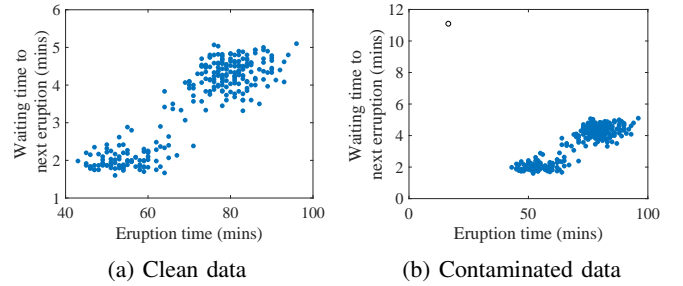


Fig. 7: Clean and contaminated versions of the Old Faithful geyser data set.

each iteration similar to the way Data-1 was generated. Most methods are able to estimate the correct number of clusters 100% of the time for the clean version of the Old Faithful data set. Our criteria, BIC_{t_3} and BIC_{Ft_3} , and BIC_{Ot_3} are insensitive to the presence of a single replacement outlier, while TBIC exhibits slight sensitivity. In the presence of an outlier, the performance of BIC_N deteriorates due to an increase in the empirical probability of overestimation. In fact, BIC_N finds 3 clusters 100% of the time. GC shows the worst performance and possesses the highest MAE.

Next, we replace a certain percentage of the Old Faithful data set with outliers and study the performance of different cluster enumeration methods. The outliers are generated from a uniform distribution over the range $[-20, 20]$ on each variate. The empirical probability of detection as a function of the percentage of replacement outliers is depicted in Fig. 8. Our criterion BIC_{Ft_3} outperforms the other methods by a considerable margin. Although BIC_{t_3} , BIC_{Ot_3} , and TBIC are able to estimate the correct number of clusters reasonably well for clean data, their performance deteriorates quickly as the percentage of outliers increases. BIC_N , X-means, and GC overestimate the number of clusters for 100% of the cases.

VII. CONCLUSION

We derived a robust cluster enumeration criterion by formulating the problem of estimating the number of clusters as

TABLE II: The performance of different cluster enumeration methods on a clean and a contaminated version of the Old Faithful data set.

		Old Faithful	Old Faithful with a single outlier
BIC _{t₃}	p_{det}	100	100
	MAE	0	0
BIC _{Ft₃}	p_{det}	100	100
	MAE	0	0
BIC _{Ot₃}	p_{det}	100	100
	MAE	0	0
TBIC [32]	p_{det}	100	92.03
	MAE	0	0.09
GC [41]	p_{det}	0	0
	MAE	10.34	10.26
BIC _N [20]	p_{det}	100	5.08
	MAE	0	1.36
X-means [10]	p_{det}	0	0
	MAE	2	2

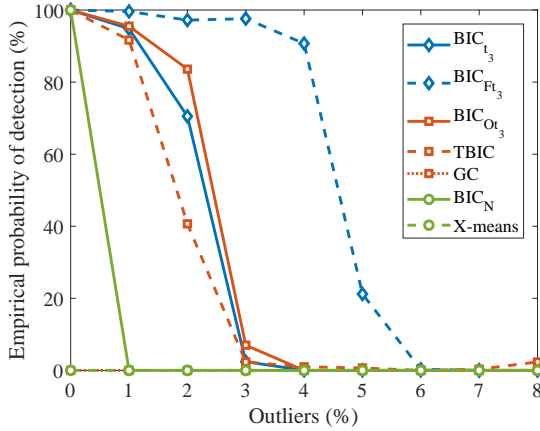


Fig. 8: Empirical probability of detection in % for the Old Faithful data set as a function of the percentage of replacement outliers.

maximization of the posterior probability of multivariate t_ν candidate models. The derivation is based on Bayes' theorem and asymptotic approximations. Further, we refined the penalty term of the robust criterion for the finite sample regime. Since both robust criteria require cluster parameter estimates as an input, we proposed a two-step cluster enumeration algorithm that uses the EM algorithm to partition the data and estimate cluster parameters prior to the calculation of either of the robust criteria. The following two statements can be made with respect to the original BIC: First, the asymptotic criterion derived specifically for cluster analysis has a different penalty term compared to the original BIC based on multivariate t_ν candidate models. Second, since the derived asymptotic criterion converges to the original BIC as data size goes to infinity, we are able to provide a justification for the use of the original BIC with multivariate t_ν candidate models. The performance of the proposed cluster enumeration algorithm is demonstrated using numerical and real data experiments. We

showed superiority of the proposed robust cluster enumeration methods in estimating the number of clusters in contaminated data sets. A possible future research direction is to represent the candidate models with a family of multivariate t_ν distributions after estimating the degree of freedom parameter ν for each cluster in each candidate model from the data.

APPENDIX A MAXIMUM LIKELIHOOD ESTIMATORS OF THE PARAMETERS OF THE MULTIVARIATE t_ν DISTRIBUTION

The log-likelihood function of the data points that belong to the m th cluster is given by

$$\begin{aligned}
 \log \mathcal{L}(\boldsymbol{\theta}_m | \mathcal{X}_m) &= \log \prod_{\mathbf{x}_n \in \mathcal{X}_m} p(\mathbf{x}_n \in \mathcal{X}_m) f(\mathbf{x}_n | \boldsymbol{\theta}_m) \\
 &= \sum_{\mathbf{x}_n \in \mathcal{X}_m} \log \left(\frac{N_m}{N} \frac{\Gamma((\nu_m + r)/2)}{\Gamma(\nu_m/2) (\pi \nu_m)^{r/2} |\boldsymbol{\Psi}_m|^{1/2}} \right. \\
 &\quad \left. \times \left(1 + \frac{\delta_n}{\nu_m} \right)^{-(\nu_m + r)/2} \right) \\
 &= N_m \log \frac{N_m}{N} + N_m \log \frac{\Gamma((\nu_m + r)/2)}{\Gamma(\nu_m/2) (\pi \nu_m)^{r/2}} \\
 &\quad - \frac{N_m}{2} \log |\boldsymbol{\Psi}_m| - \frac{(\nu_m + r)}{2} \sum_{\mathbf{x}_n \in \mathcal{X}_m} \log \left(1 + \frac{\delta_n}{\nu_m} \right), \tag{39}
 \end{aligned}$$

where $\delta_n = (\mathbf{x}_n - \boldsymbol{\mu}_m)^\top \boldsymbol{\Psi}_m^{-1} (\mathbf{x}_n - \boldsymbol{\mu}_m)$ is the squared Mahalanobis distance and $\Gamma(\cdot)$ is the gamma function. To find the maximum likelihood estimators of the centroid $\boldsymbol{\mu}_m$ and the scatter matrix $\boldsymbol{\Psi}_m$, we first derive the log-likelihood function with respect to each parameter, which results in

$$\begin{aligned}
 \frac{\partial \log \mathcal{L}(\boldsymbol{\theta}_m | \mathcal{X}_m)}{\partial \boldsymbol{\mu}_m} &= -\frac{1}{2} \sum_{\mathbf{x}_n \in \mathcal{X}_m} \frac{\nu_m + r}{\nu_m + \delta_n} \frac{d\delta_n}{d\boldsymbol{\mu}_m} \\
 &= \sum_{\mathbf{x}_n \in \mathcal{X}_m} w_n \tilde{\mathbf{x}}_n^\top \boldsymbol{\Psi}_m^{-1} \tag{40} \\
 \frac{\partial \log \mathcal{L}(\boldsymbol{\theta}_m | \mathcal{X}_m)}{\partial \boldsymbol{\Psi}_m} &= -\frac{N_m}{2} \text{Tr} \left(\boldsymbol{\Psi}_m^{-1} \frac{d\boldsymbol{\Psi}_m}{d\boldsymbol{\Psi}_m} \right) \\
 &\quad - \frac{1}{2} \sum_{\mathbf{x}_n \in \mathcal{X}_m} \frac{\nu_m + r}{\nu_m + \delta_n} \frac{d\delta_n}{d\boldsymbol{\Psi}_m} \\
 &= -\frac{N_m}{2} \boldsymbol{\Psi}_m^{-1} + \frac{1}{2} \sum_{\mathbf{x}_n \in \mathcal{X}_m} w_n \boldsymbol{\Psi}_m^{-1} \tilde{\mathbf{x}}_n \tilde{\mathbf{x}}_n^\top \boldsymbol{\Psi}_m^{-1}, \tag{41}
 \end{aligned}$$

where $\tilde{\mathbf{x}}_n = \mathbf{x}_n - \boldsymbol{\mu}_m$ and

$$w_n = \frac{\nu_m + r}{\nu_m + \delta_n} \tag{42}$$

is the weight given to \mathbf{x}_n . Then, setting Eqs. (40) and (41) to zero and simplifying the resulting expressions result in

$$\hat{\boldsymbol{\mu}}_m = \frac{\sum_{\mathbf{x}_n \in \mathcal{X}_m} w_n \mathbf{x}_n}{\sum_{\mathbf{x}_n \in \mathcal{X}_m} w_n} \tag{43}$$

$$\hat{\boldsymbol{\Psi}}_m = \frac{1}{N_m} \sum_{\mathbf{x}_n \in \mathcal{X}_m} w_n \tilde{\mathbf{x}}_n \tilde{\mathbf{x}}_n^\top. \tag{44}$$

APPENDIX B
PROOF OF THEOREM 1

Proving Theorem 1 requires finding an asymptotic approximation for $|\hat{\mathbf{J}}_m|$ in Eq. (16) and, consequently, deriving an expression for $\text{BIC}_{\nu}(M_l)$. We start the proof by taking the first derivative of the log-likelihood function, given by Eq. (39), with respect to $\boldsymbol{\theta}_m$, which results in

$$\begin{aligned} \frac{d \log \mathcal{L}(\boldsymbol{\theta}_m | \mathcal{X}_m)}{d\boldsymbol{\theta}_m} &= -\frac{N_m}{2} \text{Tr} \left(\boldsymbol{\Psi}_m^{-1} \frac{d\boldsymbol{\Psi}_m}{d\boldsymbol{\theta}_m} \right) \\ &\quad - \text{Tr} \left(\frac{(\nu_m + r)}{2} \sum_{\mathbf{x}_n \in \mathcal{X}_m} \frac{1}{\nu_m + \delta_n} \frac{d\delta_n}{d\boldsymbol{\theta}_m} \right) \\ &= -\frac{N_m}{2} \text{Tr} \left(\boldsymbol{\Psi}_m^{-1} \frac{d\boldsymbol{\Psi}_m}{d\boldsymbol{\theta}_m} \right) \\ &\quad - \frac{1}{2} \text{Tr} \left(\sum_{\mathbf{x}_n \in \mathcal{X}_m} w_n \frac{d\delta_n}{d\boldsymbol{\theta}_m} \right), \end{aligned} \quad (45)$$

where w_n is given by Eq. (42), $\tilde{\mathbf{x}}_n = \mathbf{x}_n - \boldsymbol{\mu}_m$, $\delta_n = \tilde{\mathbf{x}}_n^\top \boldsymbol{\Psi}_m^{-1} \tilde{\mathbf{x}}_n$, and

$$\frac{d\delta_n}{d\boldsymbol{\theta}_m} = -2\tilde{\mathbf{x}}_n^\top \boldsymbol{\Psi}_m^{-1} \frac{d\boldsymbol{\mu}_m}{d\boldsymbol{\theta}_m} - \tilde{\mathbf{x}}_n^\top \boldsymbol{\Psi}_m^{-1} \frac{d\boldsymbol{\Psi}_m}{d\boldsymbol{\theta}_m} \boldsymbol{\Psi}_m^{-1} \tilde{\mathbf{x}}_n. \quad (46)$$

Substituting Eq. (46) into Eq. (45) results in

$$\begin{aligned} \frac{d \log \mathcal{L}(\boldsymbol{\theta}_m | \mathcal{X}_m)}{d\boldsymbol{\theta}_m} &= -\frac{N_m}{2} \text{Tr} \left(\boldsymbol{\Psi}_m^{-1} \frac{d\boldsymbol{\Psi}_m}{d\boldsymbol{\theta}_m} \right) \\ &\quad + \text{Tr} \left(\sum_{\mathbf{x}_n \in \mathcal{X}_m} w_n \tilde{\mathbf{x}}_n^\top \boldsymbol{\Psi}_m^{-1} \frac{d\boldsymbol{\mu}_m}{d\boldsymbol{\theta}_m} \right) \\ &\quad + \frac{1}{2} \text{Tr} \left(\sum_{\mathbf{x}_n \in \mathcal{X}_m} w_n \tilde{\mathbf{x}}_n^\top \boldsymbol{\Psi}_m^{-1} \frac{d\boldsymbol{\Psi}_m}{d\boldsymbol{\theta}_m} \boldsymbol{\Psi}_m^{-1} \tilde{\mathbf{x}}_n \right) \\ &= \frac{1}{2} \text{Tr} \left(\frac{d\boldsymbol{\Psi}_m}{d\boldsymbol{\theta}_m} \boldsymbol{\Psi}_m^{-1} (\mathbf{Z}_m - N_m \boldsymbol{\Psi}_m) \boldsymbol{\Psi}_m^{-1} \right) \\ &\quad + \text{Tr} \left(\sum_{\mathbf{x}_n \in \mathcal{X}_m} w_n \tilde{\mathbf{x}}_n^\top \boldsymbol{\Psi}_m^{-1} \frac{d\boldsymbol{\mu}_m}{d\boldsymbol{\theta}_m} \right), \end{aligned} \quad (47)$$

where

$$\mathbf{Z}_m = \sum_{\mathbf{x}_n \in \mathcal{X}_m} w_n \tilde{\mathbf{x}}_n \tilde{\mathbf{x}}_n^\top. \quad (48)$$

Derivating Eq. (47), once again, with respect to $\boldsymbol{\theta}_m^\top$ results in

$$\begin{aligned} \frac{d^2 \log \mathcal{L}(\boldsymbol{\theta}_m | \mathcal{X}_m)}{d\boldsymbol{\theta}_m d\boldsymbol{\theta}_m^\top} &= \frac{1}{2} \text{Tr} \left(\frac{d\boldsymbol{\Psi}_m}{d\boldsymbol{\theta}_m} \frac{d\boldsymbol{\Psi}_m^{-1}}{d\boldsymbol{\theta}_m^\top} (\mathbf{Z}_m - N_m \boldsymbol{\Psi}_m) \boldsymbol{\Psi}_m^{-1} \right) \\ &\quad + \frac{1}{2} \text{Tr} \left(\frac{d\boldsymbol{\Psi}_m}{d\boldsymbol{\theta}_m} \boldsymbol{\Psi}_m^{-1} \left(\frac{d\mathbf{Z}_m}{d\boldsymbol{\theta}_m^\top} - N_m \frac{d\boldsymbol{\Psi}_m}{d\boldsymbol{\theta}_m^\top} \right) \boldsymbol{\Psi}_m^{-1} \right) \\ &\quad + \frac{1}{2} \text{Tr} \left(\frac{d\boldsymbol{\Psi}_m}{d\boldsymbol{\theta}_m} \boldsymbol{\Psi}_m^{-1} (\mathbf{Z}_m - N_m \boldsymbol{\Psi}_m) \frac{d\boldsymbol{\Psi}_m^{-1}}{d\boldsymbol{\theta}_m^\top} \right) \\ &\quad + \text{Tr} \left(\sum_{\mathbf{x}_n \in \mathcal{X}_m} \frac{dw_n}{d\boldsymbol{\theta}_m^\top} \tilde{\mathbf{x}}_n^\top \boldsymbol{\Psi}_m^{-1} \frac{d\boldsymbol{\mu}_m}{d\boldsymbol{\theta}_m} \right) \\ &\quad - \text{Tr} \left(\sum_{\mathbf{x}_n \in \mathcal{X}_m} w_n \frac{d\boldsymbol{\mu}_m^\top}{d\boldsymbol{\theta}_m^\top} \boldsymbol{\Psi}_m^{-1} \frac{d\boldsymbol{\mu}_m}{d\boldsymbol{\theta}_m} \right) \\ &\quad + \text{Tr} \left(\sum_{\mathbf{x}_n \in \mathcal{X}_m} w_n \tilde{\mathbf{x}}_n^\top \frac{d\boldsymbol{\Psi}_m^{-1}}{d\boldsymbol{\theta}_m^\top} \frac{d\boldsymbol{\mu}_m}{d\boldsymbol{\theta}_m} \right). \end{aligned} \quad (49)$$

From Eq. (49), the Fisher information matrix of observations from the m th cluster is given by

$$\begin{aligned} \hat{\mathbf{J}}_m &= -\frac{d^2 \log \mathcal{L}(\boldsymbol{\theta}_m | \mathcal{X}_m)}{d\boldsymbol{\theta}_m d\boldsymbol{\theta}_m^\top} \Big|_{\boldsymbol{\theta}_m = \hat{\boldsymbol{\theta}}_m} \\ &= -\frac{1}{2} \text{Tr} \left(\frac{d\boldsymbol{\Psi}_m}{d\boldsymbol{\theta}_m} \hat{\boldsymbol{\Psi}}_m^{-1} \frac{d\mathbf{Z}_m}{d\boldsymbol{\theta}_m^\top} \hat{\boldsymbol{\Psi}}_m^{-1} \right) \\ &\quad + \frac{N_m}{2} \text{Tr} \left(\frac{d\boldsymbol{\Psi}_m}{d\boldsymbol{\theta}_m} \hat{\boldsymbol{\Psi}}_m^{-1} \frac{d\boldsymbol{\Psi}_m}{d\boldsymbol{\theta}_m^\top} \hat{\boldsymbol{\Psi}}_m^{-1} \right) \\ &\quad - \text{Tr} \left(\sum_{\mathbf{x}_n \in \mathcal{X}_m} \frac{dw_n}{d\boldsymbol{\theta}_m^\top} \tilde{\mathbf{x}}_n^\top \hat{\boldsymbol{\Psi}}_m^{-1} \frac{d\boldsymbol{\mu}_m}{d\boldsymbol{\theta}_m} \right) \\ &\quad + \text{Tr} \left(\sum_{\mathbf{x}_n \in \mathcal{X}_m} w_n \frac{d\boldsymbol{\mu}_m^\top}{d\boldsymbol{\theta}_m^\top} \hat{\boldsymbol{\Psi}}_m^{-1} \frac{d\boldsymbol{\mu}_m}{d\boldsymbol{\theta}_m} \right), \end{aligned} \quad (50)$$

where w_n , $\tilde{\mathbf{x}}_n$, $\frac{dw_n}{d\boldsymbol{\theta}_m^\top}$, and $\frac{d\mathbf{Z}_m}{d\boldsymbol{\theta}_m^\top}$ are also evaluated at $\hat{\boldsymbol{\theta}}_m$, but the hat is removed for ease of notation. Note that, evaluated at $\hat{\boldsymbol{\theta}}_m$, Eq. (49) reduces to Eq. (50) because

$$\begin{aligned} \hat{\mathbf{Z}}_m - N_m \hat{\boldsymbol{\Psi}}_m &= 0 \\ \sum_{\mathbf{x}_n \in \mathcal{X}_m} w_n \tilde{\mathbf{x}}_n^\top &= 0. \end{aligned}$$

Eq. (50) can be written in a compact matrix form as

$$\hat{\mathbf{J}}_m = \begin{bmatrix} -\frac{\partial^2 \log \mathcal{L}(\hat{\boldsymbol{\theta}}_m | \mathcal{X}_m)}{\partial \boldsymbol{\mu}_m \partial \boldsymbol{\mu}_m^\top} & -\frac{\partial^2 \log \mathcal{L}(\hat{\boldsymbol{\theta}}_m | \mathcal{X}_m)}{\partial \boldsymbol{\mu}_m \partial \boldsymbol{\Psi}_m^\top} \\ -\frac{\partial^2 \log \mathcal{L}(\hat{\boldsymbol{\theta}}_m | \mathcal{X}_m)}{\partial \boldsymbol{\Psi}_m \partial \boldsymbol{\mu}_m^\top} & -\frac{\partial^2 \log \mathcal{L}(\hat{\boldsymbol{\theta}}_m | \mathcal{X}_m)}{\partial \boldsymbol{\Psi}_m \partial \boldsymbol{\Psi}_m^\top} \end{bmatrix}. \quad (51)$$

The individual elements of the block matrix in Eq. (51) are given by

$$\begin{aligned} \frac{\partial^2 \log \mathcal{L}(\hat{\boldsymbol{\theta}}_m | \mathcal{X}_m)}{\partial \boldsymbol{\mu}_m \partial \boldsymbol{\mu}_m^\top} &= \text{Tr} \left(\sum_{\mathbf{x}_n \in \mathcal{X}_m} \frac{dw_n}{d\boldsymbol{\mu}_m^\top} \tilde{\mathbf{x}}_n^\top \hat{\boldsymbol{\Psi}}_m^{-1} \frac{d\boldsymbol{\mu}_m}{d\boldsymbol{\mu}_m} \right) \\ &\quad - \text{Tr} \left(\sum_{\mathbf{x}_n \in \mathcal{X}_m} w_n \frac{d\boldsymbol{\mu}_m^\top}{d\boldsymbol{\mu}_m^\top} \hat{\boldsymbol{\Psi}}_m^{-1} \frac{d\boldsymbol{\mu}_m}{d\boldsymbol{\mu}_m} \right) \end{aligned} \quad (52)$$

$$\frac{\partial^2 \log \mathcal{L}(\hat{\boldsymbol{\theta}}_m | \mathcal{X}_m)}{\partial \boldsymbol{\mu}_m \partial \boldsymbol{\Psi}_m^\top} = \text{Tr} \left(\sum_{\mathbf{x}_n \in \mathcal{X}_m} \frac{dw_n}{d\boldsymbol{\Psi}_m^\top} \tilde{\mathbf{x}}_n^\top \hat{\boldsymbol{\Psi}}_m^{-1} \frac{d\boldsymbol{\mu}_m}{d\boldsymbol{\mu}_m} \right) \quad (53)$$

$$\begin{aligned} \frac{\partial^2 \log \mathcal{L}(\hat{\boldsymbol{\theta}}_m | \mathcal{X}_m)}{\partial \boldsymbol{\Psi}_m \partial \boldsymbol{\Psi}_m^\top} &= \frac{1}{2} \text{Tr} \left(\frac{d\boldsymbol{\Psi}_m}{d\boldsymbol{\Psi}_m} \hat{\boldsymbol{\Psi}}_m^{-1} \frac{d\mathbf{Z}_m}{d\boldsymbol{\Psi}_m^\top} \hat{\boldsymbol{\Psi}}_m^{-1} \right) \\ &\quad - \frac{N_m}{2} \text{Tr} \left(\frac{d\boldsymbol{\Psi}_m}{d\boldsymbol{\Psi}_m} \hat{\boldsymbol{\Psi}}_m^{-1} \frac{d\boldsymbol{\Psi}_m}{d\boldsymbol{\Psi}_m^\top} \hat{\boldsymbol{\Psi}}_m^{-1} \right), \end{aligned} \quad (54)$$

where

$$\frac{dw_n}{d\boldsymbol{\mu}_m^\top} = \frac{2w_n^2}{\nu_m + r} \frac{d\boldsymbol{\mu}_m^\top}{d\boldsymbol{\mu}_m^\top} \hat{\boldsymbol{\Psi}}_m^{-1} \tilde{\mathbf{x}}_n \in \mathbb{R}^{r \times 1} \quad (55)$$

$$\frac{dw_n}{d\boldsymbol{\Psi}_m^\top} = \frac{w_n^2}{\nu_m + r} \tilde{\mathbf{x}}_n^\top \hat{\boldsymbol{\Psi}}_m^{-1} \frac{d\boldsymbol{\Psi}_m}{d\boldsymbol{\Psi}_m^\top} \hat{\boldsymbol{\Psi}}_m^{-1} \tilde{\mathbf{x}}_n \in \mathbb{R}^{r \times r} \quad (56)$$

$$\frac{d\mathbf{Z}_m}{d\boldsymbol{\Psi}_m^\top} = \sum_{\mathbf{x}_n \in \mathcal{X}_m} \frac{dw_n}{d\boldsymbol{\Psi}_m^\top} \tilde{\mathbf{x}}_n \tilde{\mathbf{x}}_n^\top \in \mathbb{R}^{r^2 \times r^2}. \quad (57)$$

Note that, due to the symmetry of the Fisher information matrix, the following holds:

$$\frac{\partial^2 \log \mathcal{L}(\hat{\boldsymbol{\theta}}_m | \mathcal{X}_m)}{\partial \boldsymbol{\psi}_m \partial \boldsymbol{\mu}_m^\top} = \left(\frac{\partial^2 \log \mathcal{L}(\hat{\boldsymbol{\theta}}_m | \mathcal{X}_m)}{\partial \boldsymbol{\mu}_m \partial \boldsymbol{\Psi}_m^\top} \right)^\top \quad (58)$$

Using Eqs. (55)-(57), Eqs. (52)-(54) can be simplified to

$$\frac{\partial^2 \log \mathcal{L}(\hat{\boldsymbol{\theta}}_m | \mathcal{X}_m)}{\partial \boldsymbol{\mu}_m \partial \boldsymbol{\mu}_m^\top} = \frac{2}{\nu_m + r} \hat{\boldsymbol{\Psi}}_m^{-1} \left(\sum_{\mathbf{x}_n \in \mathcal{X}_m} w_n^2 \tilde{\mathbf{x}}_n \tilde{\mathbf{x}}_n^\top \right) \hat{\boldsymbol{\Psi}}_m^{-1} - \hat{\boldsymbol{\Psi}}_m^{-1} \sum_{\mathbf{x}_n \in \mathcal{X}_m} w_n \quad (59)$$

$$\frac{\partial^2 \log \mathcal{L}(\hat{\boldsymbol{\theta}}_m | \mathcal{X}_m)}{\partial \boldsymbol{\mu}_m \partial \boldsymbol{\Psi}_m^\top} = \frac{1}{\nu_m + r} \sum_{\mathbf{x}_n \in \mathcal{X}_m} w_n^2 \text{vec} \left(\frac{d\boldsymbol{\mu}_m}{d\boldsymbol{\mu}_m} \right)^\top \times \left(\hat{\boldsymbol{\Psi}}_m^{-1} \tilde{\mathbf{x}}_n \tilde{\mathbf{x}}_n^\top \hat{\boldsymbol{\Psi}}_m^{-1} \otimes \tilde{\mathbf{x}}_n^\top \hat{\boldsymbol{\Psi}}_m^{-1} \right) \text{vec} \left(\frac{d\boldsymbol{\Psi}_m}{d\boldsymbol{\Psi}_m^\top} \right) \quad (60)$$

$$\begin{aligned} \frac{\partial^2 \log \mathcal{L}(\hat{\boldsymbol{\theta}}_m | \mathcal{X}_m)}{\partial \boldsymbol{\Psi}_m \partial \boldsymbol{\Psi}_m^\top} &= \frac{1}{2} \text{vec} \left(\frac{d\boldsymbol{\Psi}_m}{d\boldsymbol{\Psi}_m} \right)^\top \left(\hat{\boldsymbol{\Psi}}_m^{-1} \otimes \hat{\boldsymbol{\Psi}}_m^{-1} \right) \text{vec} \left(\frac{d\mathbf{Z}_m}{d\boldsymbol{\Psi}_m^\top} \right) \\ &\quad - \frac{N_m}{2} \text{vec} \left(\frac{d\boldsymbol{\Psi}_m}{d\boldsymbol{\Psi}_m} \right)^\top \left(\hat{\boldsymbol{\Psi}}_m^{-1} \otimes \hat{\boldsymbol{\Psi}}_m^{-1} \right) \text{vec} \left(\frac{d\boldsymbol{\Psi}_m}{d\boldsymbol{\Psi}_m^\top} \right) \\ &= \frac{1}{2(\nu_m + r)} \text{vec} \left(\frac{d\boldsymbol{\Psi}_m}{d\boldsymbol{\Psi}_m} \right)^\top \left(\hat{\boldsymbol{\Psi}}_m^{-1} \otimes \hat{\boldsymbol{\Psi}}_m^{-1} \right) \\ &\quad \times \sum_{\mathbf{x}_n \in \mathcal{X}_m} w_n^2 \left(\tilde{\mathbf{x}}_n \tilde{\mathbf{x}}_n^\top \otimes \hat{\boldsymbol{\Psi}}_m^{-1} \tilde{\mathbf{x}}_n \tilde{\mathbf{x}}_n^\top \hat{\boldsymbol{\Psi}}_m^{-1} \right) \text{vec} \left(\frac{d\boldsymbol{\Psi}_m}{d\boldsymbol{\Psi}_m^\top} \right) \\ &\quad - \frac{N_m}{2} \text{vec} \left(\frac{d\boldsymbol{\Psi}_m}{d\boldsymbol{\Psi}_m} \right)^\top \left(\hat{\boldsymbol{\Psi}}_m^{-1} \otimes \hat{\boldsymbol{\Psi}}_m^{-1} \right) \text{vec} \left(\frac{d\boldsymbol{\Psi}_m}{d\boldsymbol{\Psi}_m^\top} \right). \quad (61) \end{aligned}$$

The scatter matrix $\boldsymbol{\Psi}_m$, $m = 1, \dots, l$, is a symmetric and positive definite matrix. Hence, $\text{vec}(\boldsymbol{\Psi}_m) = \mathbf{D}\mathbf{u}_m$, where $\text{vec}(\boldsymbol{\Psi}_m) \in \mathbb{R}^{r^2 \times 1}$ represents the stacking of the elements of $\boldsymbol{\Psi}_m$ into a long column vector, $\mathbf{D} \in \mathbb{R}^{r^2 \times \frac{1}{2}r(r+1)}$ denotes the duplication matrix, and $\mathbf{u}_m \in \mathbb{R}^{\frac{1}{2}r(r+1) \times 1}$ contains the unique elements of $\boldsymbol{\Psi}_m$ [65, pp. 56–57]. Taking the symmetry of the scatter matrix into account and replacing $\boldsymbol{\theta}_m$ by $\hat{\boldsymbol{\theta}}_m = [\boldsymbol{\mu}_m, \mathbf{u}_m]^\top$, Eqs. (60) and (61) simplify to

$$\begin{aligned} \frac{\partial^2 \log \mathcal{L}(\hat{\boldsymbol{\theta}}_m | \mathcal{X}_m)}{\partial \boldsymbol{\mu}_m \partial \mathbf{u}_m^\top} &= \frac{1}{\nu_m + r} \sum_{\mathbf{x}_n \in \mathcal{X}_m} w_n^2 \text{vec} \left(\frac{d\boldsymbol{\mu}_m}{d\boldsymbol{\mu}_m} \right)^\top \\ &\quad \times \left(\hat{\boldsymbol{\Psi}}_m^{-1} \tilde{\mathbf{x}}_n \tilde{\mathbf{x}}_n^\top \hat{\boldsymbol{\Psi}}_m^{-1} \otimes \tilde{\mathbf{x}}_n^\top \hat{\boldsymbol{\Psi}}_m^{-1} \right) \mathbf{D} \frac{d\mathbf{u}_m}{d\mathbf{u}_m^\top} \\ &= \frac{1}{\nu_m + r} \sum_{\mathbf{x}_n \in \mathcal{X}_m} w_n^2 \\ &\quad \times \left(\hat{\boldsymbol{\Psi}}_m^{-1} \tilde{\mathbf{x}}_n \tilde{\mathbf{x}}_n^\top \hat{\boldsymbol{\Psi}}_m^{-1} \otimes \tilde{\mathbf{x}}_n^\top \hat{\boldsymbol{\Psi}}_m^{-1} \right) \mathbf{D} \quad (62) \end{aligned}$$

$$\begin{aligned} \frac{\partial^2 \log \mathcal{L}(\hat{\boldsymbol{\theta}}_m | \mathcal{X}_m)}{\partial \mathbf{u}_m \partial \mathbf{u}_m^\top} &= \frac{1}{2(\nu_m + r)} \left(\frac{d\mathbf{u}_m}{d\mathbf{u}_m} \right)^\top \mathbf{D}^\top \left(\hat{\boldsymbol{\Psi}}_m^{-1} \otimes \hat{\boldsymbol{\Psi}}_m^{-1} \right) \\ &\quad \times \sum_{\mathbf{x}_n \in \mathcal{X}_m} w_n^2 \left(\tilde{\mathbf{x}}_n \tilde{\mathbf{x}}_n^\top \otimes \hat{\boldsymbol{\Psi}}_m^{-1} \tilde{\mathbf{x}}_n \tilde{\mathbf{x}}_n^\top \hat{\boldsymbol{\Psi}}_m^{-1} \right) \mathbf{D} \left(\frac{d\mathbf{u}_m}{d\mathbf{u}_m^\top} \right) \\ &\quad - \frac{N_m}{2} \left(\frac{d\mathbf{u}_m}{d\mathbf{u}_m} \right)^\top \mathbf{D}^\top \left(\hat{\boldsymbol{\Psi}}_m^{-1} \otimes \hat{\boldsymbol{\Psi}}_m^{-1} \right) \mathbf{D} \left(\frac{d\mathbf{u}_m}{d\mathbf{u}_m^\top} \right) \\ &= \frac{1}{2(\nu_m + r)} \mathbf{D}^\top \left(\hat{\boldsymbol{\Psi}}_m^{-1} \otimes \hat{\boldsymbol{\Psi}}_m^{-1} \right) \\ &\quad \times \sum_{\mathbf{x}_n \in \mathcal{X}_m} w_n^2 \left(\tilde{\mathbf{x}}_n \tilde{\mathbf{x}}_n^\top \otimes \hat{\boldsymbol{\Psi}}_m^{-1} \tilde{\mathbf{x}}_n \tilde{\mathbf{x}}_n^\top \hat{\boldsymbol{\Psi}}_m^{-1} \right) \mathbf{D} \\ &\quad - \frac{N_m}{2} \mathbf{D}^\top \left(\hat{\boldsymbol{\Psi}}_m^{-1} \otimes \hat{\boldsymbol{\Psi}}_m^{-1} \right) \mathbf{D}. \quad (63) \end{aligned}$$

In face of Eqs. (59), (62), and (63) three normalization factors exist, which are $\sum_{\mathbf{x}_n \in \mathcal{X}_m} w_n^2$, $\sum_{\mathbf{x}_n \in \mathcal{X}_m} w_n$, and N_m . While the relationship between $\sum_{\mathbf{x}_n \in \mathcal{X}_m} w_n^2$ and $\sum_{\mathbf{x}_n \in \mathcal{X}_m} w_n$ is non-trivial, starting from Eq. (44), and doing straight forward calculations the authors in [53] showed that

$$\sum_{\mathbf{x}_n \in \mathcal{X}_m} w_n = N_m. \quad (64)$$

As a result, we end up with only two normalization factors, namely $\sum_{\mathbf{x}_n \in \mathcal{X}_m} w_n^2$ and N_m . Given that $l \ll N$, $N \rightarrow \infty$ indicates that $\epsilon \rightarrow \infty$, where $\epsilon = \max(\sum_{\mathbf{x}_n \in \mathcal{X}_m} w_n^2, N_m)$. Hence, as $N \rightarrow \infty$

$$\left| \frac{1}{\epsilon} \hat{\mathbf{J}}_m \right| \approx \mathcal{O}(1), \quad (65)$$

where $\mathcal{O}(1)$ denotes Landau's term which tends to a constant as $N \rightarrow \infty$. Using the result in Eq. (65), Eq. (16) can be simplified to

$$\begin{aligned} \log p(M_l | \mathcal{X}) &\approx \log p(M_l) + \sum_{m=1}^l \log \left(f(\hat{\boldsymbol{\theta}}_m | M_l) \mathcal{L}(\hat{\boldsymbol{\theta}}_m | \mathcal{X}_m) \right) \\ &\quad + \frac{lq}{2} \log 2\pi - \frac{1}{2} \sum_{m=1}^l \log \left| \epsilon \frac{\hat{\mathbf{J}}_m}{\epsilon} \right| + \rho \\ &= \log p(M_l) + \sum_{m=1}^l \log \left(f(\hat{\boldsymbol{\theta}}_m | M_l) \mathcal{L}(\hat{\boldsymbol{\theta}}_m | \mathcal{X}_m) \right) \\ &\quad + \frac{lq}{2} \log 2\pi - \frac{q}{2} \sum_{m=1}^l \log \epsilon - \frac{1}{2} \sum_{m=1}^l \log \left| \frac{\hat{\mathbf{J}}_m}{\epsilon} \right| + \rho, \quad (66) \end{aligned}$$

where $q = \frac{1}{2}r(r+3)$ is the number of estimated parameters per cluster.

Assume that

(A.7) $p(M_l)$ and $f(\hat{\boldsymbol{\theta}}_l | M_l)$ are independent of the data length N .

Ignoring the terms in Eq. (66) that do not grow as $N \rightarrow \infty$ results in

$$\begin{aligned} \text{BIC}_{t_\nu}(M_l) &\triangleq \log p(M_l | \mathcal{X}) \\ &\approx \sum_{m=1}^l \log \mathcal{L}(\hat{\boldsymbol{\theta}}_m | \mathcal{X}_m) - \frac{q}{2} \sum_{m=1}^l \log \epsilon + \rho. \quad (67) \end{aligned}$$

Substituting the expression of $\log \mathcal{L}(\hat{\boldsymbol{\theta}}_m | \mathcal{X}_m)$, given by Eq. (39), into Eq. (67) results in

$$\begin{aligned} \text{BIC}_{t_\nu}(M_l) &= \sum_{m=1}^l N_m \log N_m - N \log N - \sum_{m=1}^l \frac{N_m}{2} \log |\hat{\boldsymbol{\Psi}}_m| \\ &\quad + \sum_{m=1}^l N_m \log \frac{\Gamma((\nu_m + r)/2)}{\Gamma(\nu_m/2) (\pi \nu_m)^{r/2}} \\ &\quad - \frac{1}{2} \sum_{m=1}^l \sum_{\mathbf{x}_n \in \mathcal{X}_m} (\nu_m + r) \log \left(1 + \frac{\delta_n}{\nu_m} \right) \\ &\quad - \frac{q}{2} \sum_{m=1}^l \log \epsilon + \rho. \quad (68) \end{aligned}$$

Finally, ignoring the model independent terms in Eq. (68) results in Eq. (18). This concludes the proof.

APPENDIX C

CALCULATION OF THE DETERMINANT OF THE FISHER INFORMATION MATRIX

The Fisher information matrix, given by Eq. (51), is a block matrix and its determinant is calculated as

$$|\hat{\mathbf{J}}_m| = \left| -\frac{\partial^2 \log \mathcal{L}(\hat{\boldsymbol{\theta}}_m | \mathcal{X}_m)}{\partial \boldsymbol{\mu}_m \partial \boldsymbol{\mu}_m^\top} + \frac{\partial^2 \log \mathcal{L}(\hat{\boldsymbol{\theta}}_m | \mathcal{X}_m)}{\partial \boldsymbol{\mu}_m \partial \mathbf{u}_m^\top} \right. \\ \times \left(\frac{\partial^2 \log \mathcal{L}(\hat{\boldsymbol{\theta}}_m | \mathcal{X}_m)}{\partial \mathbf{u}_m \partial \mathbf{u}_m^\top} \right)^{-1} \left. \frac{\partial^2 \log \mathcal{L}(\hat{\boldsymbol{\theta}}_m | \mathcal{X}_m)}{\partial \mathbf{u}_m \partial \boldsymbol{\mu}_m^\top} \right| \\ \times \left| -\frac{\partial^2 \log \mathcal{L}(\hat{\boldsymbol{\theta}}_m | \mathcal{X}_m)}{\partial \mathbf{u}_m \partial \mathbf{u}_m^\top} \right|, \quad (69)$$

where $\frac{\partial^2 \log \mathcal{L}(\hat{\boldsymbol{\theta}}_m | \mathcal{X}_m)}{\partial \boldsymbol{\mu}_m \partial \boldsymbol{\mu}_m^\top}$, $\frac{\partial^2 \log \mathcal{L}(\hat{\boldsymbol{\theta}}_m | \mathcal{X}_m)}{\partial \boldsymbol{\mu}_m \partial \mathbf{u}_m^\top}$, and $\frac{\partial^2 \log \mathcal{L}(\hat{\boldsymbol{\theta}}_m | \mathcal{X}_m)}{\partial \mathbf{u}_m \partial \mathbf{u}_m^\top}$ are given by Eqs. (59), (62), and (63), respectively.

APPENDIX D

VECTOR AND MATRIX DIFFERENTIATION RULES

The numerator layout of derivatives is used in proving Theorem 1. Given that $\mathbf{y} \in \mathbb{R}^{p \times 1}$ and $\mathbf{Y} \in \mathbb{R}^{p \times p}$, we have used the following matrix and vector differentiation rules (see [65] for details):

$$\frac{d}{d\mathbf{y}} \mathbf{y}^\top \mathbf{y} = 2\mathbf{y}^\top \quad (70)$$

$$\frac{d}{d\mathbf{Y}} \mathbf{Y}^{-1} = -\mathbf{Y}^{-1} \frac{d\mathbf{Y}}{d\mathbf{Y}} \mathbf{Y}^{-1} \quad (71)$$

$$\frac{d}{d\mathbf{Y}} \log |\mathbf{Y}| = \text{Tr} \left(\mathbf{Y}^{-1} \frac{d\mathbf{Y}}{d\mathbf{Y}} \right) \quad (72)$$

We have also exploited properties of the trace (Tr) and vec operators. Given matrices \mathbf{A} , \mathbf{B} , \mathbf{C} , and \mathbf{D} with matching dimensions, the following hold true:

$$\text{Tr}(\mathbf{AB}) = \text{Tr}(\mathbf{BA}) \quad (73)$$

$$\frac{d}{d\mathbf{A}} \text{Tr}(\mathbf{A}) = \text{Tr} \left(\frac{d\mathbf{A}}{d\mathbf{A}} \right) \quad (74)$$

$$\frac{d \text{Tr}(\mathbf{BA})}{d\mathbf{B}} = \text{Tr} \left(\frac{d\mathbf{B}}{d\mathbf{B}} \mathbf{A} \right) = \text{Tr} \left(\frac{d\mathbf{B}}{d\mathbf{B}} \right) \mathbf{A} = \mathbf{A} \quad (75)$$

$$\text{Tr}(\mathbf{A}^\top \mathbf{CDB}^\top) = \text{vec}(\mathbf{A})^\top (\mathbf{B} \otimes \mathbf{C}) \text{vec}(\mathbf{D}) \quad (76)$$

$$\text{vec}(\mathbf{ABC}) = (\mathbf{C}^\top \otimes \mathbf{A}) \text{vec}(\mathbf{B}) \quad (77)$$

$$\text{vec} \left(\frac{d\mathbf{A}}{d\mathbf{A}} \right) = \frac{d}{d\mathbf{A}} \text{vec}(\mathbf{A}) \quad (78)$$

ACKNOWLEDGMENT

This work is supported by the LOEWE initiative (Hessen, Germany) within the NICER project. The work of F. K. Teklehaymanot is supported by the ‘Excellence Initiative’ of the German Federal and State Governments and the Graduate School of Computational Engineering at Technische Universität Darmstadt. The work of M. Muma is supported by the ‘Athene Young Investigator Programme’ of Technische Universität Darmstadt.

REFERENCES

- [1] L. Kaufman and P. J. Rousseeuw, *Finding Groups in Data: An Introduction to Cluster Analysis*. John Wiley & Sons, Inc, 1990.
- [2] R. S. King, *Cluster Analysis and Data Mining: An Introduction*. Mercury Learning and Information, 2015.
- [3] R. N. Davé and R. Krishnapuram, “Robust clustering methods: a unified view,” *IEEE Transactions on Fuzzy Systems*, vol. 5, no. 2, pp. 270–293, 1997.
- [4] R. Xu and D. Wunsch, “Survey of clustering algorithms,” *IEEE Transactions on Neural Networks*, vol. 16, no. 3, pp. 645–678, 2005.
- [5] J. C. Dunn, “A fuzzy relative of the ISODATA process and its use in detecting compact well-separated clusters,” *Journal of Cybernetics*, vol. 3, no. 3, pp. 32–57, 1973.
- [6] D. L. Davies and D. W. Bouldin, “A cluster separation measure,” *IEEE Transactions on Pattern Analysis and Machine Intelligence*, vol. PAMI-1, no. 2, pp. 224–227, 1979.
- [7] T. Caliński and J. Harabasz, “A dendrite method for cluster analysis,” *Communications in Statistics*, vol. 3, no. 1, pp. 1–27, 1974.
- [8] P. J. Rousseeuw, “Silhouettes: a graphical aid to the interpretation and validation of cluster analysis,” *Journal of Computational and Applied Mathematics*, vol. 20, no. 1, pp. 53–65, 1987.
- [9] R. Tibshirani, G. Walther, and T. Hastie, “Estimating the number of clusters in a dataset via the gap statistic,” *Journal of the Royal Statistical Society Series B*, vol. 63, no. 2, pp. 411–423, 2001.
- [10] D. Pelleg and A. Moore, “X-means: extending K-means with efficient estimation of the number of clusters,” in *Proceedings of the 17th International Conference on Machine Learning (ICML)*, Stanford, USA, 2000, pp. 727–734.
- [11] A. Kalogeratos and A. Likas, “Dip-means: an incremental clustering method for estimating the number of clusters,” in *Advances in Neural Information Processing Systems 25*, 2012, pp. 2402–2410.
- [12] G. Hamerly and E. Charles, “Learning the K in K-means,” in *Proceedings of the 16th International Conference on Neural Information Processing Systems (NIPS)*, Whistler, Canada, 2003, pp. 281–288.
- [13] Y. Feng and G. Hamerly, “PG-means: learning the number of clusters in data,” in *Advances in Neural Information Processing Systems 19*, 2007, pp. 393–400.
- [14] C. Constantinopoulos, M. K. Titsias, and A. Likas, “Bayesian feature and model selection for Gaussian mixture models,” *IEEE Transactions on Pattern Analysis and Machine Intelligence*, vol. 28, no. 6, pp. 1013–1018, 2006.
- [15] T. Huang, H. Peng, and K. Zhang, “Model selection for Gaussian mixture models,” *Statistica Sinica*, vol. 27, no. 1, pp. 147–169, 2017.
- [16] A. Mehrjou, R. Hosseini, and B. N. Araabi, “Improved Bayesian information criterion for mixture model selection,” *Pattern Recognition Letters*, vol. 69, pp. 22–27, 2016.
- [17] W. J. Krzanowski and Y. T. Lai, “A criterion for determining the number of groups in a data set using sum-of-squares clustering,” *Biometrics*, vol. 44, no. 1, pp. 23–34, 1988.
- [18] Q. Zhao and P. Fränti, “WB-index: a sum-of-squares based index for cluster validity,” *Data & Knowledge Engineering*, vol. 92, pp. 77–89, 2014.
- [19] F. K. Teklehaymanot, M. Muma, J. Liu, and A. M. Zoubir, “In-network adaptive cluster enumeration for distributed classification/labeling,” in *Proceedings of the 24th European Signal Processing Conference (EU-SIPCO)*, Budapest, Hungary, 2016, pp. 448–452.
- [20] F. K. Teklehaymanot, M. Muma, and A. M. Zoubir, “Bayesian cluster enumeration criterion for unsupervised learning,” *IEEE Transactions on Signal Processing*, vol. 66, no. 20, pp. 5392–5406, 2018.
- [21] —, “Novel Bayesian cluster enumeration criterion for cluster analysis with finite sample penalty term,” in *Proceedings of the 43rd IEEE International Conference on Acoustics, Speech and Signal Processing (ICASSP)*, Calgary, Canada, 2018, pp. 4274–4278.
- [22] O. Arbelaitz, I. Gurrutxaga, J. Muguerza, J. M. Pérez, and I. Perona, “An extensive comparative study of cluster validity indices,” *Pattern Recognition*, vol. 46, no. 1, pp. 243–256, 2013.
- [23] G. W. Milligan and M. C. Cooper, “An examination of procedures for determining the number of clusters in a data set,” *Psychometrika*, vol. 50, no. 2, pp. 159–179, 1985.
- [24] U. Maulik and S. Bandyopadhyay, “Performance evaluation of some clustering algorithms and validity indices,” *IEEE Transactions on Pattern Analysis and Machine Intelligence*, vol. 24, no. 12, pp. 1650–1654, 2002.
- [25] M. Halkidi, Y. Batistakis, and M. Vazirgiannis, “On clustering validation techniques,” *Journal of Intelligent Information Systems*, vol. 17, no. 2/3, pp. 107–145, 2001.

- [26] M. T. Gallegos and G. Ritter, "A robust method for cluster analysis," *The Annals of Statistics*, vol. 33, no. 1, pp. 347–380, 2005.
- [27] L. A. García-Escudero, A. Gordaliza, C. Matrán, and A. Mayo-Isacar, "Exploring the number of groups in robust model-based clustering," *Statistics and Computing*, vol. 21, no. 4, pp. 585–599, 2011.
- [28] A. M. Zoubir, V. Koivunen, Y. Chakhchoukh, and M. Muma, "Robust estimation in signal processing," *IEEE Signal Processing Magazine*, vol. 29, no. 4, pp. 61–80, 2012.
- [29] A. M. Zoubir, V. Koivunen, E. Ollila, and M. Muma, *Robust Statistics for Signal Processing*. Cambridge University Press, 2018.
- [30] P. Binder, M. Muma, and A. M. Zoubir, "Robust and adaptive diffusion-based classification in distributed networks," *EURASIP Journal on Advances in Signal Processing*, vol. 2016, no. 34, pp. 1–13, 2016.
- [31] M. Wang, Z. B. Abrams, S. M. Kornblau, and K. R. Coombes, "Thresher: determining the number of clusters while removing outliers," *BMC Bioinformatics*, vol. 19, no. 9, pp. 1–15, 2018.
- [32] N. Neykov, P. Filzmoser, R. Dimova, and P. Neytchev, "Robust fitting of mixtures using the trimmed likelihood estimator," *Computational Statistics & Data Analysis*, vol. 52, no. 1, pp. 299–308, 2007.
- [33] M. T. Gallegos and G. Ritter, "Trimming algorithms for clustering contaminated grouped data and their robustness," *Advances in Data Analysis and Classification*, vol. 3, no. 2, pp. 135–167, 2009.
- [34] —, "Using combinatorial optimization in model-based trimmed clustering with cardinality constraints," *Computational Statistics & Data Analysis*, vol. 54, no. 3, pp. 637–654, 2010.
- [35] C. Fraley and A. Raftery, "How many clusters? Which clustering method? Answers via model-based cluster analysis," *The Computer Journal*, vol. 41, no. 8, pp. 578–588, 1998.
- [36] A. Dasgupta and A. E. Raftery, "Detecting features in spatial point processes with clutter via model-based clustering," *Journal of the American Statistical Association*, vol. 93, no. 441, pp. 294–302, 1998.
- [37] J. L. Andrews and P. D. McNicholas, "Model-based clustering, classification, and discriminant analysis via mixtures of multivariate t -distributions," *Statistics and Computing*, vol. 22, no. 5, pp. 1021–1029, 2012.
- [38] P. D. McNicholas and S. Subedi, "Clustering gene expression time course data using mixtures of multivariate t -distributions," *Journal of Statistical Planning and Inference*, vol. 142, no. 5, pp. 1114–1127, 2012.
- [39] H. Frigui and R. Krishnapuram, "A robust algorithm for automatic extraction of an unknown number of clusters from noisy data," *Pattern Recognition Letters*, vol. 17, no. 12, pp. 1223–1232, 1996.
- [40] Y. Hu, C. Zou, Y. Yang, and F. Qu, "A robust cluster validity index for fuzzy c -means clustering," in *Proceedings of the International Conference on Transportation, Mechanical, and Electrical Engineering (TMEE)*, Changchun, China, 2011, pp. 448–451.
- [41] P. Binder, M. Muma, and A. M. Zoubir, "Gravitational clustering: a simple, robust and adaptive approach for distributed networks," *Signal Processing*, vol. 149, pp. 36–48, 2018.
- [42] K.-L. Wu, M.-S. Yang, and J.-N. Hsieh, "Robust cluster validity indexes," *Pattern Recognition*, vol. 42, no. 11, pp. 2541–2550, 2009.
- [43] E. Zemene, Y. T. Tesfaye, A. Prati, and M. Pelillo, "Simultaneous clustering and outlier detection using dominant sets," in *Proceedings of the 23rd International Conference on Pattern Recognition (ICPR)*, Cancún, Mexico, 2016, pp. 2325–2330.
- [44] L. Ott, L. Pang, F. Ramos, and S. Chawla, "On integrated clustering and outlier detection," in *Advances in Neural Information Processing Systems 27*, 2014, pp. 1359–1367.
- [45] L. A. García-Escudero, A. Gordaliza, C. Matrán, and A. Mayo-Isacar, "A review of robust clustering methods," *Advances in Data Analysis and Classification*, vol. 4, no. 2–3, pp. 89–109, 2010.
- [46] G. Schwarz, "Estimating the dimension of a model," *The Annals of Statistics*, vol. 6, no. 2, pp. 461–464, 1978.
- [47] G. J. McLachlan and D. Peel, "Robust cluster analysis via mixtures of multivariate t -distributions," *Amin A., Dori D., Pudil P., and Freeman H. (Eds.), Lecture Notes in Computer Science*, vol. 1451, pp. 658–666, 1998.
- [48] D. Peel and G. J. McLachlan, "Robust mixture modelling using the t distribution," *Statistics and Computing*, vol. 10, pp. 339–348, 2000.
- [49] S. Kotz and S. Nadarajah, *Multivariate t Distributions and Their Applications*. Cambridge university press, 2004.
- [50] K. L. Lange, R. J. A. Little, and J. M. G. Taylor, "Robust statistical modeling using the t distribution," *Journal of the American Statistical Association*, vol. 84, no. 408, pp. 881–896, 1989.
- [51] C. Liu and D. Rubin, "ML estimation of the t distribution using EM and its extensions, ECM and ECME," *Statistica Sinica*, vol. 5, pp. 19–39, 1995.
- [52] B. Kibria and A. Joarder, "A short review of multivariate t -distribution," *Journal of Statistical Research*, vol. 40, no. 1, pp. 59–72, 2006.
- [53] J. T. Kent, D. E. Tyler, and Y. Vard, "A curious likelihood identity for the multivariate t -distribution," *Communications in Statistics - Simulations and Computation*, vol. 23, no. 2, pp. 441–453, 1994.
- [54] J. E. Cavanaugh and A. A. Neath, "Generalizing the derivation of the Schwarz information criterion," *Communication in Statistics - Theory and Methods*, vol. 28, no. 1, pp. 49–66, 1999.
- [55] P. M. Djurić, "Asymptotic MAP criteria for model selection," *IEEE Transactions on Signal Processing*, vol. 46, no. 10, pp. 2726–2735, 1998.
- [56] P. Stoica and Y. Selen, "Model-order selection: a review of information criterion rules," *IEEE Signal Processing Magazine*, vol. 21, no. 4, pp. 36–47, 2004.
- [57] T. Ando, *Bayesian Model Selection and Statistical Modeling*. Chapman & Hall/CRC, 2010.
- [58] R. A. Maronna, "Robust M -estimators of multivariate location and scatter," *The Annals of Statistics*, vol. 4, no. 1, pp. 51–67, 1976.
- [59] S. Nadarajah and S. Kotz, "Estimation methods for the multivariate t distribution," *Acta Applicandae Mathematicae*, vol. 102, no. 1, pp. 99–118, 2008.
- [60] C. R. Rao and Y. Wu, "A strongly consistent procedure for model selection in a regression problem," *Biometrika*, vol. 76, no. 2, pp. 369–74, 1989.
- [61] A. J. Izenman, *Modern Multivariate Statistical Techniques: Regression, Classification, and Manifold Learning*. Springer Science+Business Media, LLC, 2008.
- [62] A. Azzalini and A. W. Bowman, "A look at some data on the Old Faithful geyser," *Applied Statistics*, vol. 39, no. 3, pp. 357–365, 1990.
- [63] C. M. Bishop, *Pattern Recognition and Machine Learning*. Springer Science+Business Media, LLC, 2006.
- [64] C. Hennig, "Clusters, outliers, and regression: fixed point clusters," *Journal of Multivariate Analysis*, vol. 86, no. 1, pp. 183–212, 2003.
- [65] J. R. Magnus and H. Neudecker, *Matrix Differential Calculus with Applications in Statistics and Econometrics (3 ed.)*. John Wiley & Sons Ltd, 2007.